Seakeeping calculations with FineMarine

Auteur : Plaza Mendoza, David Andres
Promoteur(s) : 14928
Faculté : Faculté des Sciences appliquées
Diplôme : Master : ingénieur civil mécanicien, à finalité spécialisée en "Advanced Ship Design"
Année académique : 2020-2021
URI/URL : http://hdl.handle.net/2268.2/13508

Seakeeping calculations with FineMarine

submitted on 26 August 2021

by

PLAZA MENDOZA David Andres | 13 Rue Pitre Chevalier | 44000 Nantes | davidplazam@hotmail.com

Student ID No.: 200529N (ECN) | S193104 (ULG)

First Reviewer:

Alban Leroyer

Assistant Professor - École Centrale de Nantes

1 Rue de la Noë

44300 Nantes

France

Second Reviewer:

Antoine Ducoin

Associate Professor - École Centrale de Nantes

1 Rue de la Noë

44300 Nantes

France

With the support of the Erasmus+ Programme of the European Union

CONTENTS

LIST OF FIGURES

LIST OF TABLES

DECLARATION OF AUTHORSHIP

I declare that this thesis and the work presented in it are my own and have been generated by me as the result of my own original research.

Where I have consulted the published work of others, this is always clearly attributed.

Where I have quoted from the work of others, the source is always given. With the exception of such quotations, this thesis is entirely my own work.

I have acknowledged all main sources of help.

Where the thesis is based on work done by myself jointly with others, I have made clear exactly what was done by others and what I have contributed myself.

This thesis contains no material that has been submitted previously, in whole or in part, for the award of any other academic degree or diploma.

I cede copyright of the thesis in favour of the École Centrale de Nantes

Date: 25/08/2021 Signature: David Andrés Plaza Mendoza

ABSTRACT

Using computational fluid dynamics (CFD), Seakeeping tests aim to obtain the ship's response, avoiding or validating experimental tests. Still, this conventional process is costly in computational time, even with supercomputers. Fortunately, applying an infinite number of superimposed harmonic factors, Transient Wave Group (TWG) facilitates to reduce simulation time, using the Gaussian wave packages model recommended by Clauss and Bergmann in 1986. This project uses FineMarine (CFD software) to evaluate simulation with TWG in three steps of simulations. The first stage is dealing with 2D simulations without any solid to verify the input wave generation. The followed step includes the response measurement of a mid-ship section in beam seas. Finally, the seakeeping response evaluation of an 80 meters patrol boat in beam and head seas in 3D dimension.

The results generated by the simulation have a level of acceptance. For the first stage (TWG without solid body), the simulation obtains the input proposed spectrum and free surface elevation (FSE). In the step with the midsection, the results became acceptable but with certain discrepancies due to lack of simulation time due to the low value of roll inertia which generates prolonged movement. As the last stage, the results differences disappeared with the 3D model in head seas due to the high inertia value incidence in pitch motion. In general, inertia helps to obtain fast response stability. In addition, ship velocity seakeeping simulations in head seas assert the use of TWG compared to experimental data and Qship potential flow solver.

Conventional seakeeping test takes long simulations for irregular waves such as JONSWAP, ITTC, Pierson-Moskovitz. Otherwise, for a regular wave, it is manageable but not efficient in terms of acquisition data. That is why TWG is a method to optimize the simulation time in terms of irregular waves. Overall, TWG is splendidly suited for ships on Head Seas, with values close to experimental. However, using TWG in beam seas requires a longer simulation time until its movements stabilize, even with low wave steepness wave excitation.

1. INTRODUCTION

The seakeeping test is an experimental or numerical process responsible for obtaining the response amplitude operator (RAO), which forms the basis in the ship design stage. Experimental tests generate demanding money process whit the risk of model scale effect (non-accurate fully scaled ship responses). More precisely, it uses irregular waves of phases of random characteristics. Those tests require a long simulation time to obtain acceptable results. Besides, potential flow solvers (as Qship) have faster results but Froud number of restrictions. On the other hand (avoiding costs), the experimental test can be replicated by numerical simulation. Still, the computational time increases so significantly (even with supercomputers) that it can be a restriction in the design stage. For this reason, the current primary objective is the reduction of the seakeeping simulation time for an 80 meters Patrol Boat using FineMarine CFD software. Then it is convenient to use an irregular wave model with a deterministic phase that can cover the total energy obtained in the random or statistical model.

TWG is one example of deterministic model phases, which generates a short simulation time compared to the time needed by random phase or statistical models. Figure 1 shows an example of reducing the number of iterations between the conventional JONSWAP and the spectrum generated by the TWG. The reduction of the number of iterations is evident, which leads to the conclusion that, in general, the statistical model must have a large to recover good results in the energy imposed by the wave generation. Therefore, this work aims to validate TWG seakeeping simulations tests in a patrol boat by comparing experimental results in wave tank and Qship potential flow solver.

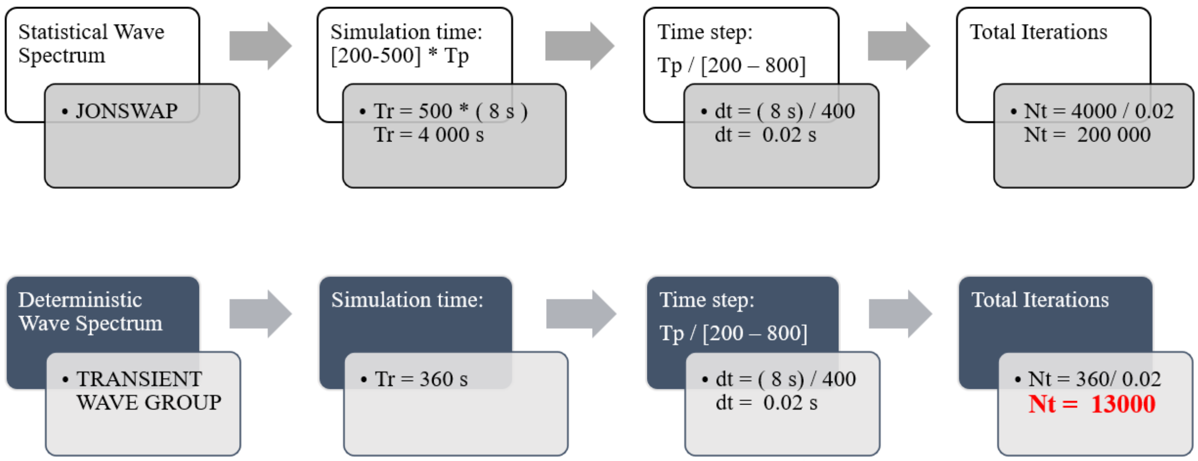

Figure 1. Conventional and deterministic wave spectrums comparison in a seakeeping test

2. LITERATURE REVIEW

The TWG model was developed over time since the stochastic method to determine the response of marine structures takes long simulations to generate accurate results. Davis and Zarnick [1] were the firsts to introduce a transient wave to obtain spectrum energy in the frequencies of interest in experimental model tests. Following this work, Takesawa [2] creates a model with the desired input spectrum to produce transient waves through a wave generator and an experimental model test. The improvement occurs after Clauss plus Bergman, during 1986 [3], includes a Gaussian Wave Package to control TWG shape.

Even though experimental tests use this method, TWG fits perfectly in numerical methods. With this, it can solve the time constrain of the conventional seakeeping simulations. Currently, Mousaviraad and Carrica [4] in 2010 made Unsteady Reynolds average Navier-Stokes (URANS) simulations of TWG with a simplified model referred to the proposed in [3], with successful results. In addition, the model was used in Open FOAM as a source to do the simulation. However, in the current project, the TWG used is the proposed by Clauss in 1986 [3] and implemented in a FineMarine CFD (marine NUMECA software)

3. METHODOLOGY

Figure 2 summarizes the obtention of RAO of ship vessels using a TWG in a simulation. The process starts creating the theory of TWG and the equivalent energy spectrum and phase using a time-discrete Fourier transform procedure using python code. Besides, the corresponding energy precedent of the TWG must have enough energy in a frequency range where the ship may respond. Finally, FineMarine uses this wave energy excitation to achieve the ship response in the seakeeping simulation.

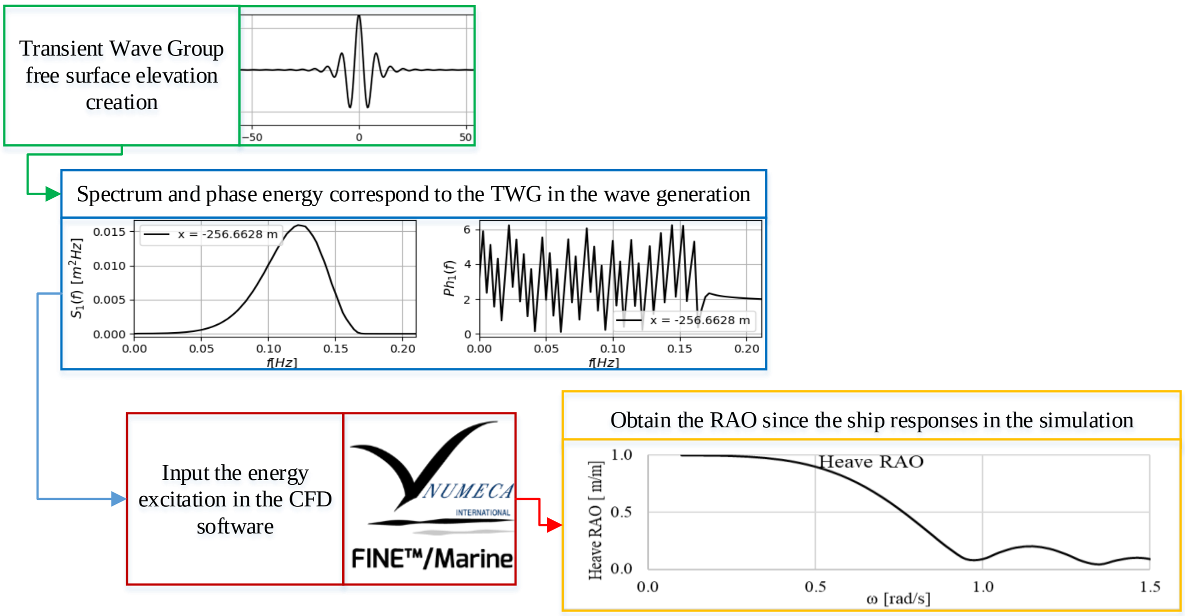

Figure 2. Seakeeping simulation summary using TWG

As a result, the simulation provides a time-domain signal of the FSE and the ship motions. The signal concerning the FSE must reach the input TWG related to the input energy of the excitation. Besides, the responses obtained are roll, heave, and pitch depending on the simulation environment (head seas or beam seas). Finally in Eq. 1 shows the RAO for each ship movement using a calculation python code of spectrum (S) in the FSE and ship responses signals [5].

$$\left|RAO_{roll\ or\ heave\ or\ pitch}\right|^2 = \frac{S_{roll\ or\ heave\ or\ pitch}}{S_{FSE}} \tag{1}$$

Consequently, Figure 3 shows the proposal stages of simulations to assert the use of TWG in the seakeeping test in FineMarine. The first stage aims to verify the theory of Transient Wave Group and the spectrum generator python code with the numerical simulation using FineMarine. The second stage is to determine in a simplified 2D midship section model the response amplitude operator subjected at different periods of TWG and after compared with regular waves simulations. Additionally, the last stage is accurate 3D patrol boat simulation subjected at the beam and head seas TWG. These values are compared with results using Qship software (Potential flow solver) and the experimental data of real-time simulation in irregular waves.

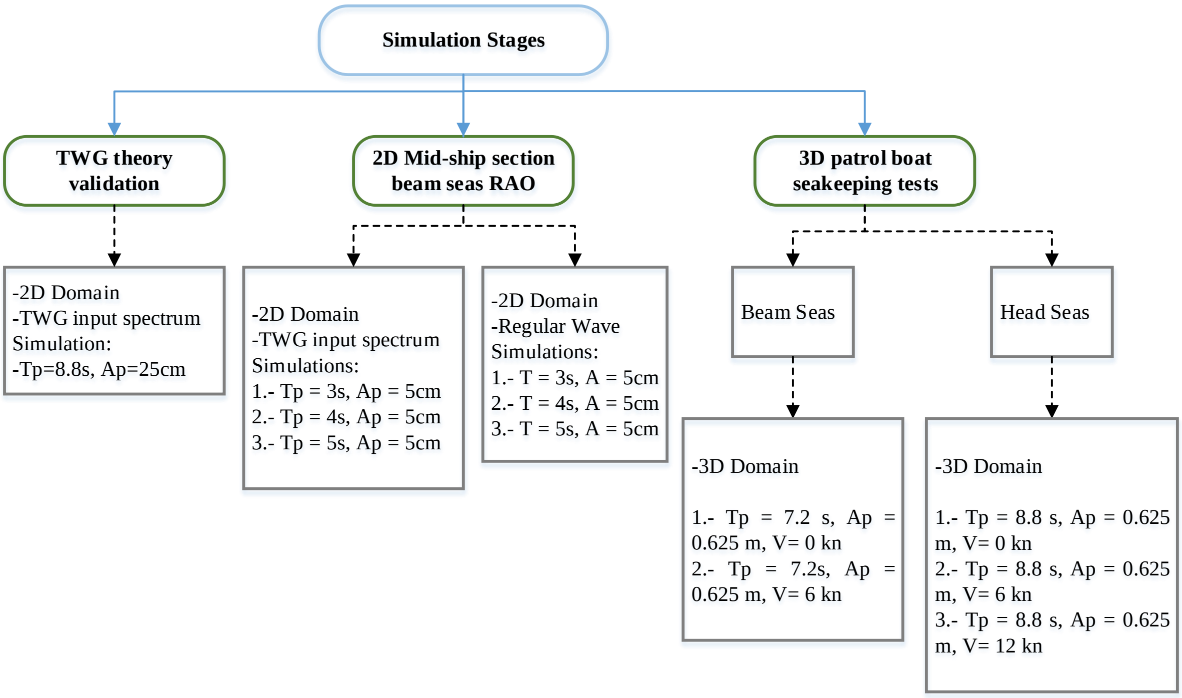

Figure 3. Simulation stages in the present project

4. TRANSIENT WAVE GROUP MODEL

The method to create a TWG by [3] is shown in Eq. 2. It results from a composition of an infinite number of superimposed harmonic factors, but three components can condense it. The first component, X_1, is the damping effect in the system, Eq. 3. The second component, X_2, is the modulation term, Eq. 4. Finally, the third component, X_3, represents the harmonic term shown in Eq. 5.

$$\eta\,(x, t) = a_0 \cdot X_1 \cdot X_2 \cdot X_3 \tag{2}$$

$$X_1 = \sqrt[4]{\frac{1}{1+s^4B^2t^2}} \tag{3}$$

$$X_2 = \exp\left[-\frac{1}{2}\cdot\frac{s^2}{1+s^4B^2t^2}\cdot(x-At)^2\right] \tag{4}$$

$$X_3 = \cos\left(k_0x-\omega_0t\ +\frac{\mathrm{arctg}(-s^2Bt)}{2}+\frac{1}{2}\cdot\frac{s^2Bt}{1+s^4B^2t^2}\cdot(x-At)^2\right) \tag{5}$$

The main wavenumber (k_0) and wave amplitude (a_0), in addition to a standard deviation (s), produce the required energy spectrum. Also, the equations present the coefficients A (Eq. 6) and B (Eq. 7), which represent the group velocity and damping factor, respectively. In addition, the equation the phase velocity, C_0, is presented in Eq. 8.

$$A = \frac{C_0}{2}\cdot\left(1+\frac{2k_0d}{\sinh(2k_0d)}\right) \tag{6}$$

$$B = \frac{C_0}{2}\cdot d\cdot\left[\frac{1-2k_0d\cdot\coth(2k_0d)}{\sinh(2k_0d)}-\frac{1}{2\sinh(2k_0d)}\cdot\left(\frac{\sinh(2k_0d)}{2k_0d}-\frac{2k_0d}{\sinh(2k_0d)}\right)\right] \tag{7}$$

$$C_0 = \sqrt{\frac{g}{k_0}\cdot\tanh(k_0d)} \tag{8}$$

Figure 4 shows the desired FSE shape in the concentrated point (longitudinal center of gravity of the ship), which is the primary purpose of the TWG design. Nevertheless, it is essential to mention that shape is established in *x* and *t* equal to cero. Following the exact Figure 4, the ship in the point of the longitudinal center of gravity will receive the transient wave at a time of 150 seconds.

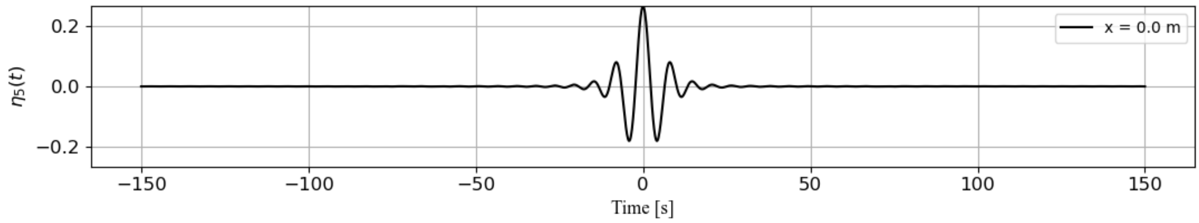

Figure 4. Transient wave group at the concentrated point

4.1. TWG design

The design of a transient wave group uses python code as program language, and the procedure follows limited steps to raise a final design. First, with the desired peak period and wave amplitude, it proceeds to modify two factors:

- Wave standard deviation, *S*
- Total time simulation, *T*

However, before changing the variables to the design, plotting the FSE in different locations altogether is recommended. One point is in the position of the wave generation; this position is vital because these waves generated are the input data in FineMarine. The second point is on the ship-longitudinal center of gravity or concentrated point ($x = 0$ and $t = 0$) because the desired wave shape in time follows the structure of Figure 4. Besides, the methodology to obtain the spectrum from the FSE is through Discrete Fourier Transform (DFT) developed in python open-source code.

In general, the procedure to modify the values is to design a TWG with the desired wave shape in the concentration point and equal spectrum in each position in the study.

Therefore, as an example of TWG design, Figure 5 shows the lecture points correspond to the wave generation point and the concentrated point (location of the ship). In addition, the figure shows a transient wave of 8.8 seconds of peak period and a wave amplitude of 0.266 meters. Using a time simulation of 80 seconds and a standard deviation of 0.1 does not have the desired shape in the concentrated point, and all the spectrums are different.

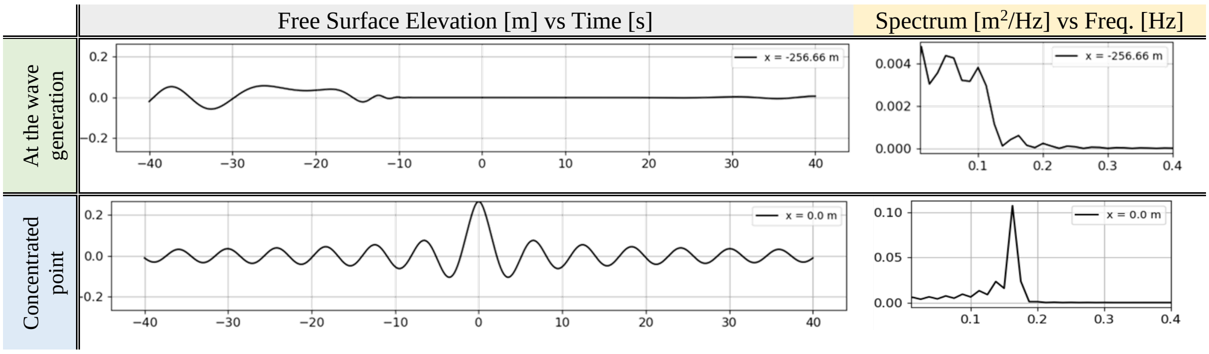

Figure 5. Transient wave group: First iteration, s = 0.1 and T = 80 s

Consequently, the second iteration of the design is shown in Figure 6, where it is appreciated a change of standard deviation of 0.03. As a result of this change, the FSE shape at the concentration point is correct; therefore, this is the final selected standard deviation. Even with the desired shape in the concentrated point, the result must change because the spectrums are not equal in the two points. That is why a shift in time simulation and time step can handle this inequality of spectrums.

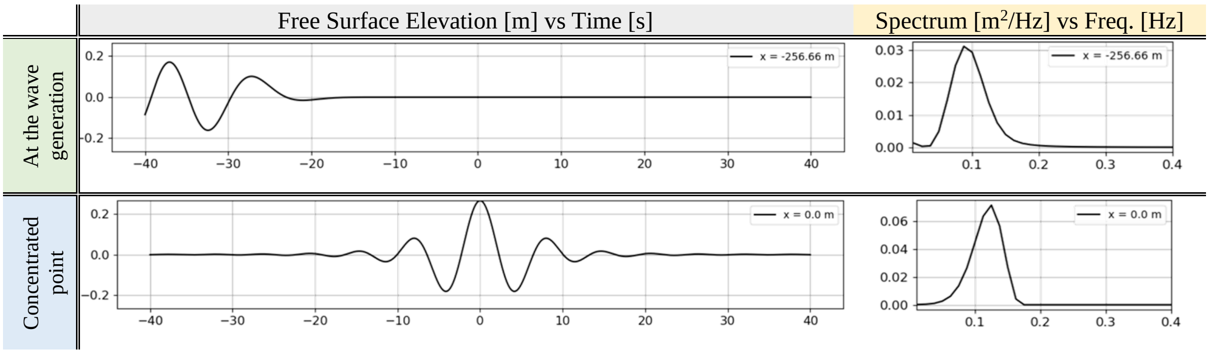

Figure 6. Transient wave group: Second iteration, s = 0.03 and T = 80 s

As the final iteration, the effect of increased time simulation at 300 seconds is showed in Figure 7. The final shapes and spectrums are correct for the design input spectrum in FineMarine. One comment is that the final time (in this TWG case) is the minimum time needed to create equal energy in the whole domain. It is possible to increase the time if required. Finally, it is recommendable to use a small wave steepness (<<1) to avoid any presence of non-linearities.

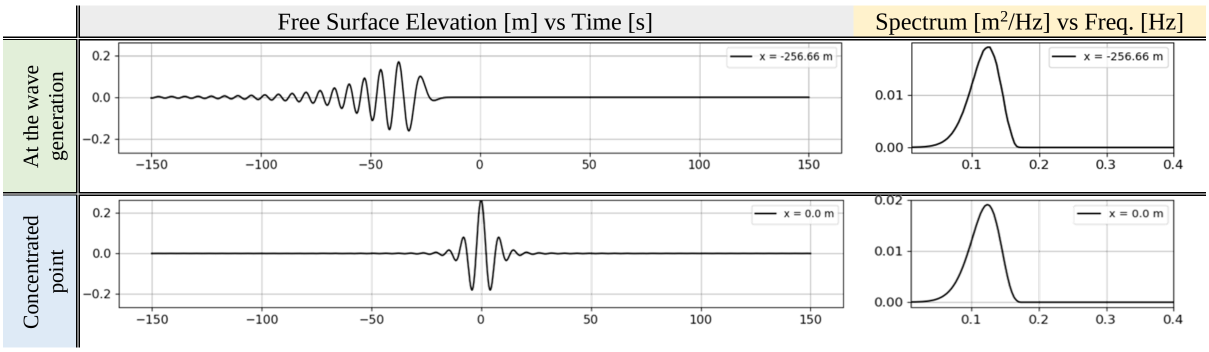

Figure 7. Transient wave group: Last iteration, s = 0.03 and T = 300 s

5. FINEMARINE

FineMarine is software created by NUMECA company, which is in charge of performing simulations of CFD. FineMarine may perform simulation in the fields of resistance, maneuvering, seakeeping, and others. In the current project, is used the recommendations presented by the NUMECA documentation platform [6]. Generally, FineMarine comprises three basic modules to generate the mesh, run the simulation, and visualize the post-processing process results, in Figure 8.

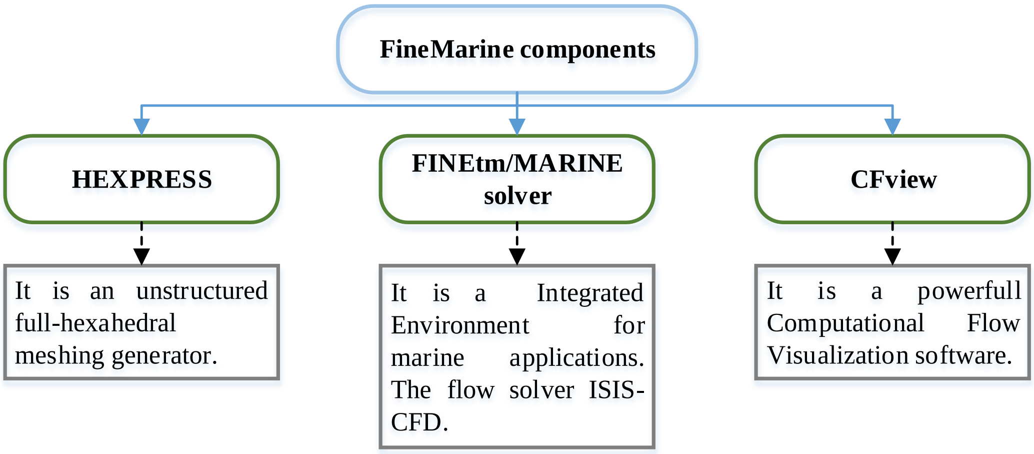

Figure 8. Components of the FineMarine software

5.1. HEXPRESS

This module of FineMarine is in charge of generating the mesh ushing hexagonal elements, either in 2D and 3D models. Also, the whole problem depends on what field is studied (seakeeping, resistance, and others). Still, every mesh in HEXPRESS follows the steps shown in Figure 9. In general, the process starts with the desired domain with the solid to proceed at setup all the refinements in the ship solid walls and finishing with the insertion of viscous mesh to capture the boundary layer.

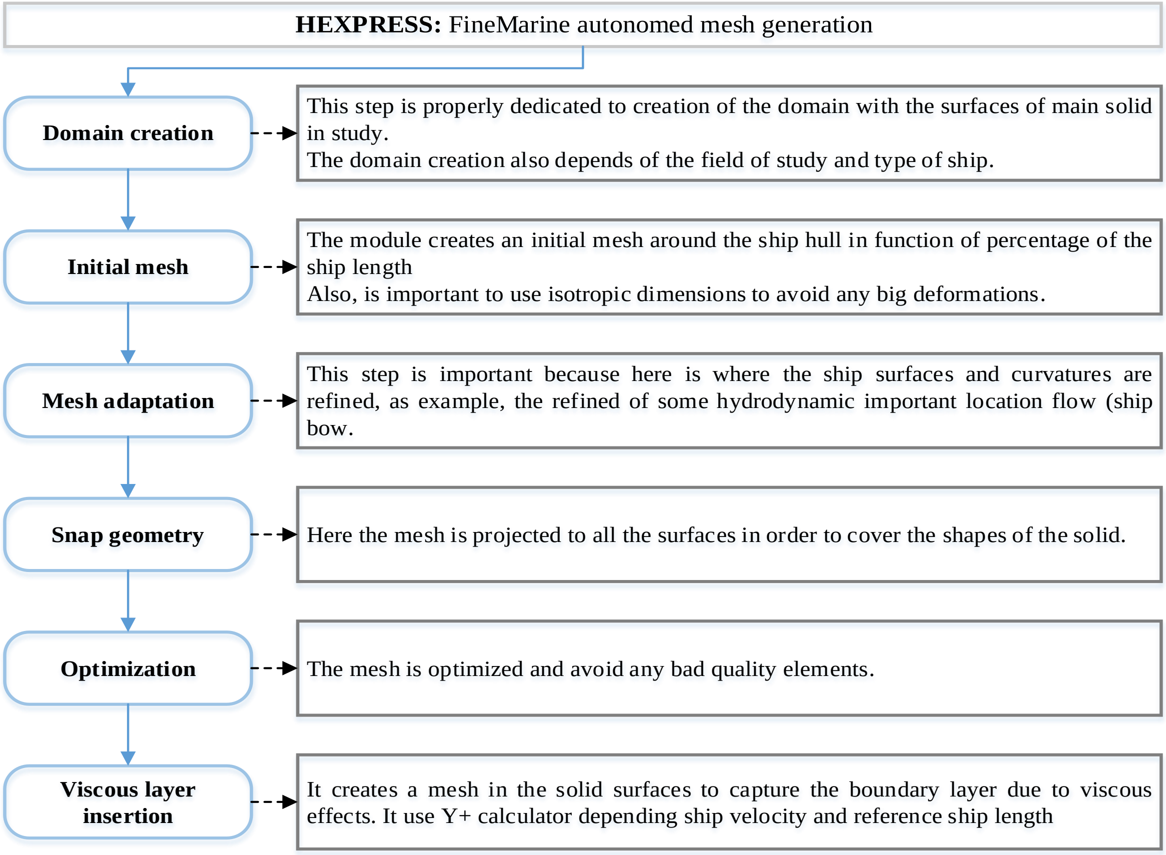

Figure 9. Mesh creation step in HEXPRESS

Furthermore, mesh quality reflects accuracy in the solver; that is why the evaluation of these parameters must be behind the running simulation. The quality grid parameters that HEXPRESS shown and considered in this project are:

- Negative Cells: Avoid these cells that generate negative volume. In general, the module FINE^{TM}/MARINE is not able to start the simulation with these cells.
- Concave cells – Twisted Cells: Avoid these cells that have robustness issues. In the mesh, optimization notices the presence of this cell.
- Orthogonality: These cell parameters must be considered in a case to avoid any not deformed cell. In the present project, the minimum angle required is 10 degrees to ensure quality results in the simulation.

5.2. FINE^{TM}/MARINE solver

This module operates to start since the mesh of the problem passes all the quality evaluations. Here is applied all the physical setup to perform any Hydrodynamic application. The solver's name is ISIS-CFD (developed by the Ecole Centrale de Nantes and CNRS) which uses incompressible unsteady Reynolds-average Navier Stokes equations (RANSE). Concerning spatial discretization, the solver uses the finite volume method on the transport equations.

The RANSE equations are composed of two sets of equations:

- Momentum conservations equations: The velocity field is derived from these equations.
- Mass conservation constraints or continuity equations: The pressure field is extracted from these equations.

In addition, extra transport equations must model turbulent flows with a similar form to solve and discretize as the momentum equations. In the present project turbulence model used is k-ω SST which NUMECA recommends in seakeeping tests.

5.3. CFView

CFView is a software that allows obtaining visualization results from the previous simulation obtained by ISIS solver. The software will enable us to show the flows characteristic of the test, such as the mass fraction, velocity field, and pressure field. This software is essential because it helps interpret the results using pictures or videos of the hydrodynamic application.

5.4. Seakeeping setup

The domain setup used in this project is based on the guidelines for boundary condition wave generators on the online documentation platform of FineMarine [6]. In the following simulations, it can be performed in 2D as well 3D runs. In addition, the boundaries conditions in seakeeping tests are wave generator in the limitation on the left, hydrostatic pressure on top and bottom edges, a far-field in the right boundary, and finally, mirror in the side boundaries as shown in Figure 10.

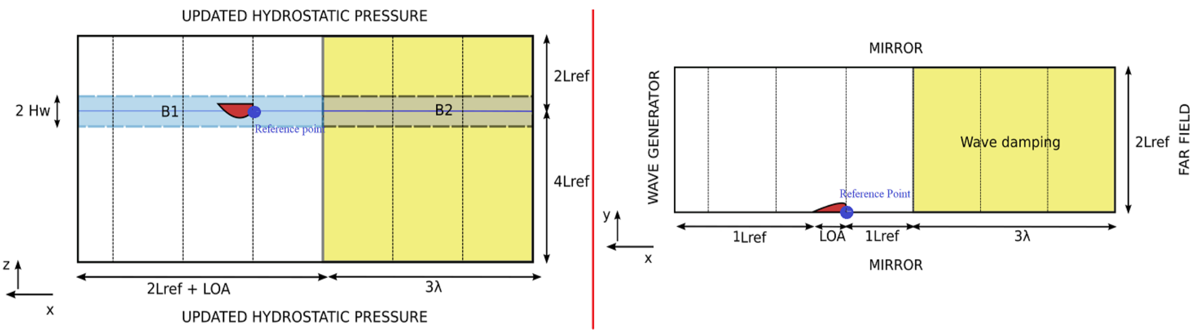

Figure 10. 3D view of the boundaries and domain conditions in Seakeeping tests

From the previous figure, it is crucial to recall three aspects:

- The sector B1 is a refinement mesh to capture the FSE. Also, it has a range of two times the wave high in case of any wave concentration.

- The sector B2 is a course damping mesh dedicate to dissipate waves and avoid reflection waves in the simulation.
- The yellow sector is dedicated to the additional setup model, using the wave damping model (based on Darcy's law to damp the momentum in the Z direction).
- L_{REF} is the maximum distance between the ship length and wavelength.

The critical points in the simulation setup are summarized in Table 1 [6]. The vital part is that the time step used depends on the peak period used in TWG simulation. Besides, the wave generation boundary condition is where the desired TWG is set with a data file (frequency, spectrum, and phase angle), as shown in Figure 11. Otherwise, if the wave generation is regular or irregular behavior, only the characteristic of the wave generation (depth, period, and wave amplitude).

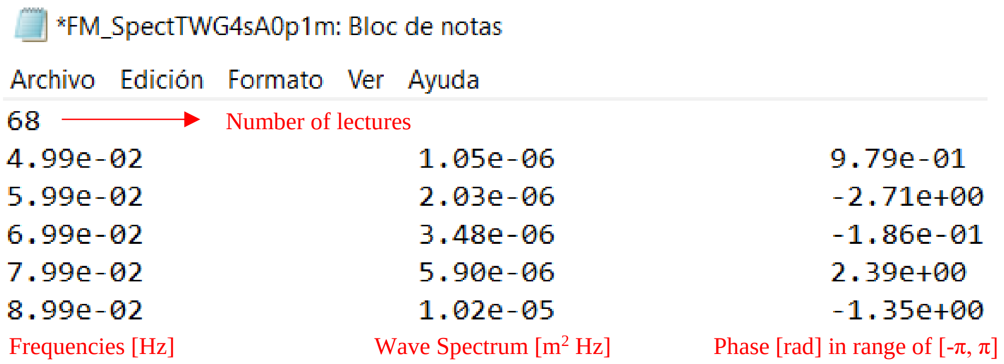

Figure 11. Input transient wave group data file example (User-defined wave generation)

Table 1. Simulation setup in FineMarine seakeeping tests [6]

Physical Configuration	
General Parameters	Time configuration: Unsteady
Fluid Model	Multifluid
Flow Model	Turbulence model: k-omega (SST-Menter)
Boundary Conditions	Inlet patch: Wave Generator, Regular, Irregular, and **User-defined** Side patches: Mirror plane Top and Bottom: Update hydrostatic pressure Ship: Slip wall in the deck otherwise Wall-function
Body motion	Tx0 (Surge): Imposed with motion law: 1/2 Sinusoidal Ramp Tz0 (Heave): Motion type Solved Ry1 (Pitch): Motion type: Solved
Additional Model	
Wave damping	Activate wave generation
Numerical Model	
Numerical Models	Activate velocity clipping: Factor 10
Computational Control	
Time step	dt = T / 200
Convergence	Number of non-linear iterations: 16-20 Converge Criteria: 4 orders Activate the Transpiration method
Expert parameters	Expert parameter WeightCoefModifLaw_: *3 0.85*

6. FIRST STAGE: 2D-TWG THEORY VALIDATION

The principal aim of this stage is to verify the creation of the proposed FSE in the FineMarine time signal. The domain used in the consequence's simulation follows the guidelines in FineMarine for a wave period of 8.8 seconds and a wave amplitude of 27 cm (Table 2), and a deviation standard of 0.03 m^{-1}. In addition, the proposed FSE and the equivalent spectrum are shown in Figure 12, where it is essential to mention that the distance between the wave generation and the concentrated point is 256 meters.

Table 2. Numerical wave tank in FineMarine setup parameters

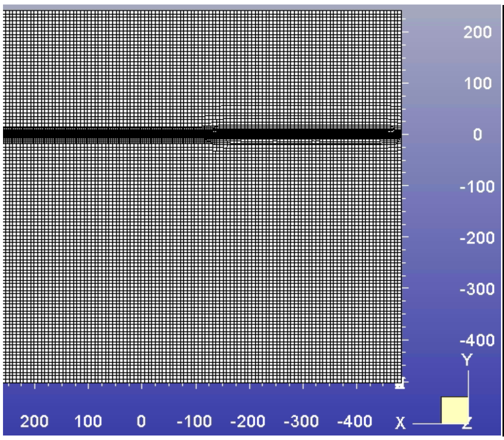

Input Data		
T_p	8.8	[s]
λ_w	120.8	[m]
H_w	0.532	[m]
L_{ref}	120.8	[m]

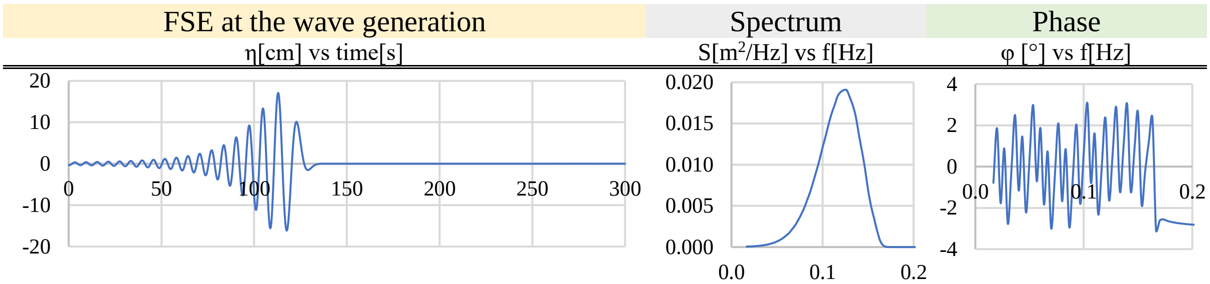

Figure 12. Input Spectrum TWG at stage 1 to assert TWG theory validation

6.1. Simulation Results

The results were not precisely the input spectrum due to phase angle (φ_C), which creates a gap in the time signal. Figure 13 shows in the first row the gap between the FineMarine time signal (in red) and the theory TWG (in black) in the wave generation. The exact figure has shown the result of adding a gap angle in the input phase spectrum. After all, the results have the same behavior with a gap angle of -90 degrees because FineMarine is working with sine angle wave generation instead of cosine as the theory.

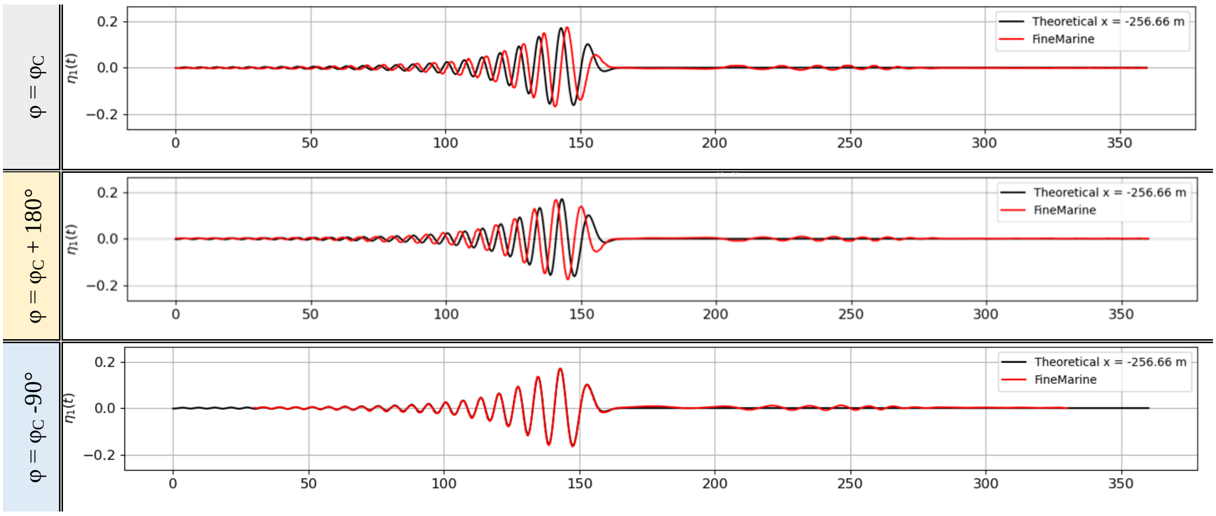

Figure 13. Phase angle gap incidence in the FSE time signal at the wave generation

Finally, with the solved phase gap problem, the simulation in FineMarine has the same shape as the theory. Figure 14 shows the results of the two probes (the first probe in the wave generation and the second in the concentration point). The simulation time signal follows either the FSE or the spectrum theory but with neglected fluctuation.

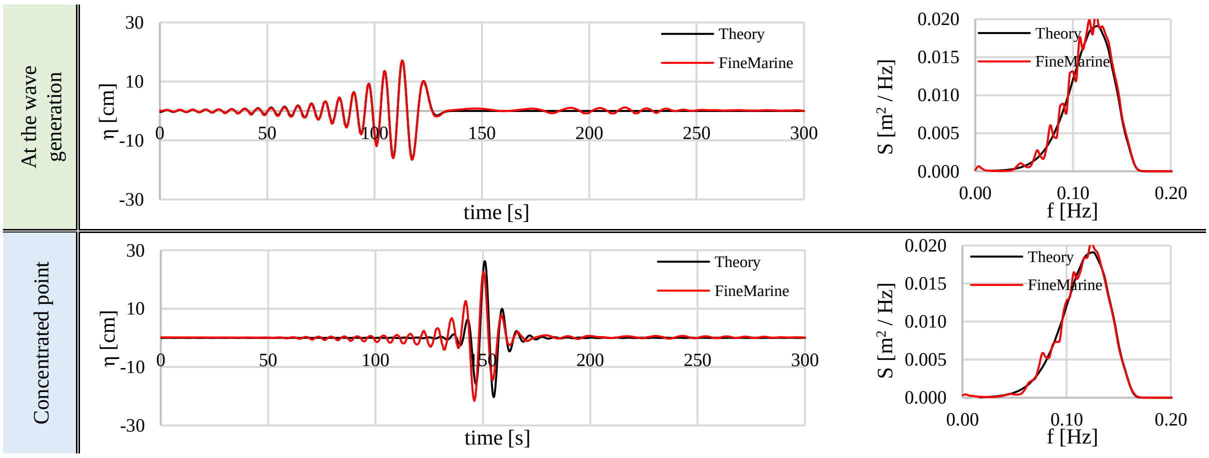

Figure 14. Transient wave group simulation comparison

6.2. Accuracy Evaluation

The time signal obeys the theory FSE and the input spectrum. However, the presence of fluctuations, the simulation deserved to measure the accuracy of the spectrum. Altogether, the critical value for accuracy is the spectrum because this value is required to obtain the RAO (Eq. 1). For this, the normalized root mean square error proposed by Windt et al. [7] calculates the accuracy in a finite number of waves (N, or the number of frequencies lectures). The normalized root mean square error ($nRMSE(x_n)$) uses the theoretical input spectrum (S_t) and the time signal spectrum (S). Also, it depends on the position (x_n) where the spectrum is measured (Eqs. 9-10).

$$nRMSE(x_n)=\frac{RMSE(x_n)}{max(S_t(f_i))}\cdot 100\% \tag{9}$$

$$RMSE(x_n)=\sqrt{\frac{\sum_{i=1}^{N}[S(x_n,f_i)-S_t(f_i)]^2}{N}} \tag{10}$$

The present simulation of this stage measured the accuracy wave spectrum in five probes located in the mesh domain. Table 3 shows the position of each and the mean normalized root mean error of the spectrum. The results show errors of less than 5%, which is minimum. However, the simulation improved with time signal manipulation seen in the next section, 6.3.

Table 3. Normalized root mean square error in wave spectrum at different x position

Probes Position [m]				
P1: Wave Generation	P2	P3	P4: Concentrated point	P5
267.61	146.81	26	10.95	0
Normalized Root Mean Square Error [%]				
4.74	3.06	2.82	2.94	3.01

6.3. Time signal manipulation (post-processing data)

In the last section, the fluctuation in the signal data creates an error in the generated spectrum. The filtering method used to solve the error is the Hann window function as a recommendation by Mousaviraad [4] due to spectral leakage. The Hann window [8] (*w(n)*) is a coefficient to get smooth the discontinuities at the beginning (*n=1*) and the end of the sample signal (*n=N*), as is shown in Eq. 11 and Figure 15.

$$w(n)=0.5-0.5\cos\left(\frac{2\pi n}{N-1}\right) \tag{11}$$

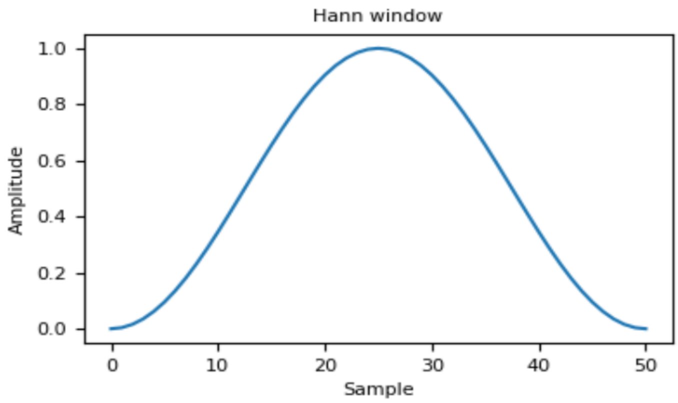

Figure 15. Hann window coefficient for a signal of 50 samples *[8]*

The Hann window is applied to the concentrated point (in FSE and future simulation ship responses). Figure 16 shows the comparison of the spectrum on the concentrated point after the use Hann window filter in the FSE. The shape is smoother than the spectrum without filtering. Finally, the accuracy by normalized root means square passes from 2.94 % to 2.15%, which improves the obtention of RAO values.

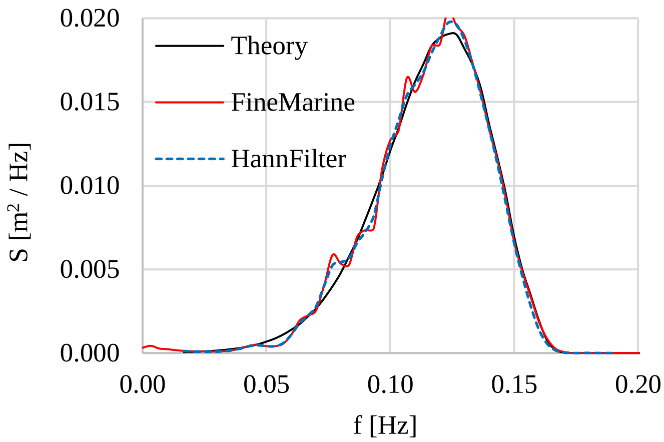

Figure 16. Spectrum Hann filter comparison

Therefore, filtering is required in the FSE time signal results and the responses as Pitch, Heave, and Roll in the future sections. The mean reason is that the filtering helps obtain smooth results and the decreased error. One final comment is that theory TWG has acceptable results even though the FSE time signal fluctuations are evident. However, it still has enough energy to create a ship response and, in consequence, obtain RAO results.

7. SECOND STAGE: 2D – MIDSHIP SECTION RESPONSE

Since the previous section validates the TWG production, the new assessment asserts the responses in a mid-ship area obtained in regular waves (RW) and the acquired in TWG wave excitation. Using 2D cases follows the computational time gained due to less computational power and easy setup. On the other hand, asserting the solid simulations in 3D cases take more effort in computational literature. The simulation is recreating beam seas simulation, which leads to comparing the roll and heave RAO. The mid-ship section used, Table 4, has one chine, and it does not account for bilge keel. Besides, the hydrostatic and inertia matrix details are presented in Table 4, an input body motion in FineMarine.

Table 4. Mid-ship section Hydrostatics

Section details		
B	7.3	[m]
T	1.33	[m]
Δ	6072.5	[kg]
K_G	2.798	[m]
K_B	0.817	[m]
B_{MT}	4.3	[m]
I_{xx}	3.964E+04	[kg m²]

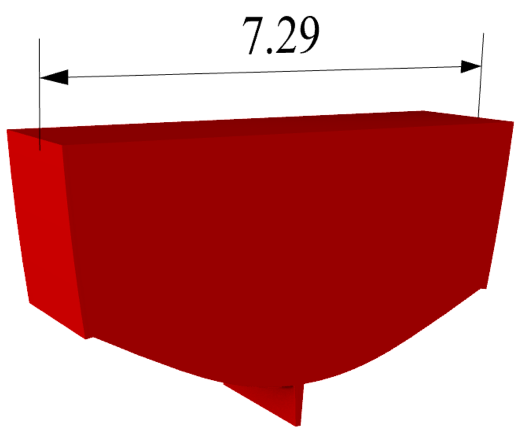

In general, it is compared the RAO results with different periods of TWG with the same amplitude. In addition, simulation with different peaks periods and a fixed period to determine if the same RAO is not dependent on the amplitude. Besides, all the simulations are compared and verified with the result at different simulations in RW. Table 5 shows all the simulations performed in this stage.

Table 5. Simulation list on Mid-ship section

Simulation	Type	T_p [s]	A_o [m]	s [m^{-1}]
1	TWG	3	0.05	0.2
2	TWG	4	0.05	0.12
3	TWG	5	0.05	0.085
4	TWG	4	0.1	0.12
5	TWG	4	0.5	0.12
6, 7, 8	RW	3, 4, 5	0.05	-

Consequently, the input spectrum is shown in Figure 17. In addition, the figure shows the comparison between the period (3, 4, 5 s) and the wave amplitude (0.05, 0.1, 0.5 m). The drastic change of energy is appreciated when the amplitude is changed. Still, in any case, this number is delicate because with a low number is possible to reduce problems of non-linearities in the solution.

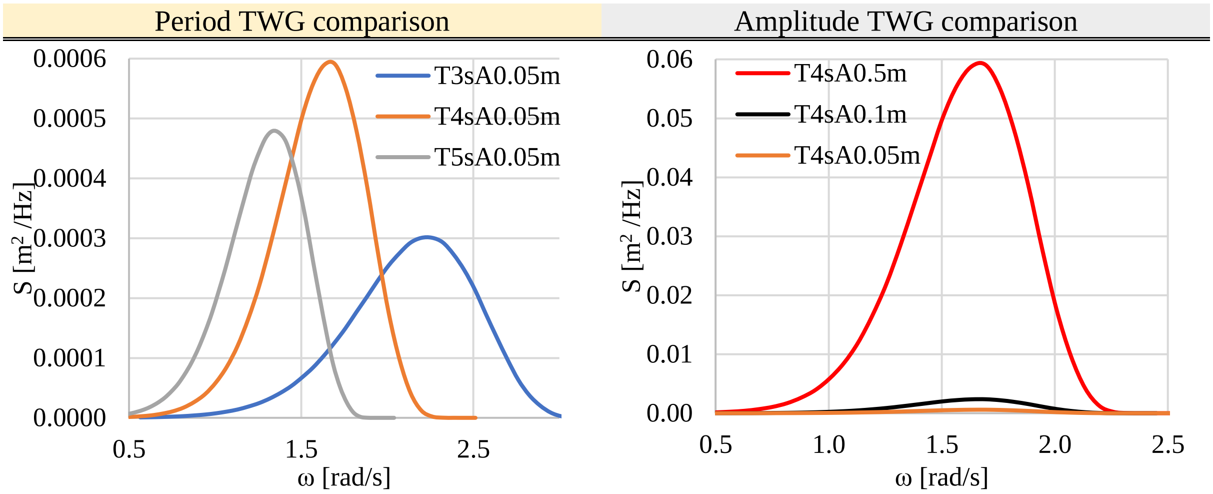

Figure 17. Transient wave group input spectrum for stage 2 simulations

7.1. CFD mid-ship section

This stage has different domain creation in comparison with the other stages. The setup follows the guidelines for internal wave generator (IWG) on the online documentation platform of FineMarine [6]. The change of boundary wave generation to internal wave generation is for the treatment of the wave reflections created by the solid side. In summary, a far-field in the boundary along the wave generation must be selected (Figure 18). Also, the characteristic of the input waves does it in the additional physics model of internal wave generation.

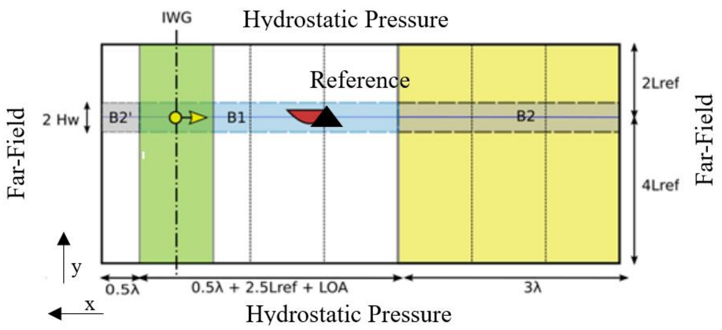

Figure 18. 2D view of the boundaries conditions and domain

To continue with the reference of the previous figure, the following Table 6 shown the domain obtained with the corresponding ship and wave characteristics. The same table represents 4 seconds of wave period and 0.5 meters of wave amplitude. However, the domains changes depending on the design wave characteristics in the input spectrum.

Table 6. Internal wave tank in FineMarine setup parameters

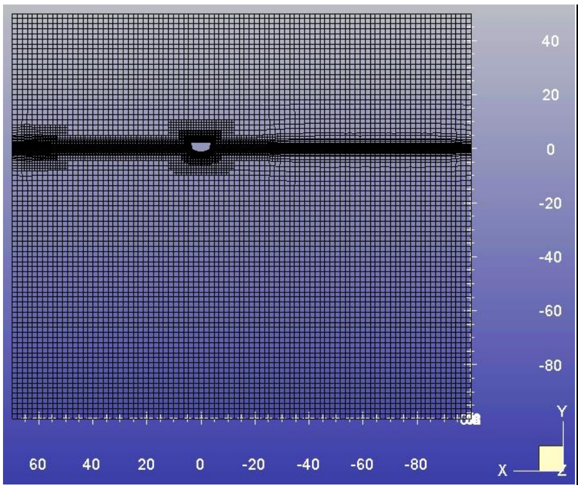

Input Data		
B_{OA}	7.3	[m]
T_p	4.0	[s]
λ_w	25	[m]
H_w	1.0	[m]
L_{ref}	25	[m]

7.1.1. *Wave Damping tools*

The HEXPRESS software, in this case, the mesh is made to damp the wave changing the size of the longitudinal cells. In consequence, the wave is not captured and damped, as is shown in Figure 19 a. Besides, FineMarine has a particular model selecting a domain sector where the waves are damped, as shown in Figure 19 b. Therefore, the damping tools in the position nearest to the wave generation dissipate the reflected waves caused by the ship's solid side. On the other hand, the damping tools eliminate the reflected wave in the far-field.

a. Mesh Damping — b. Damping additional model

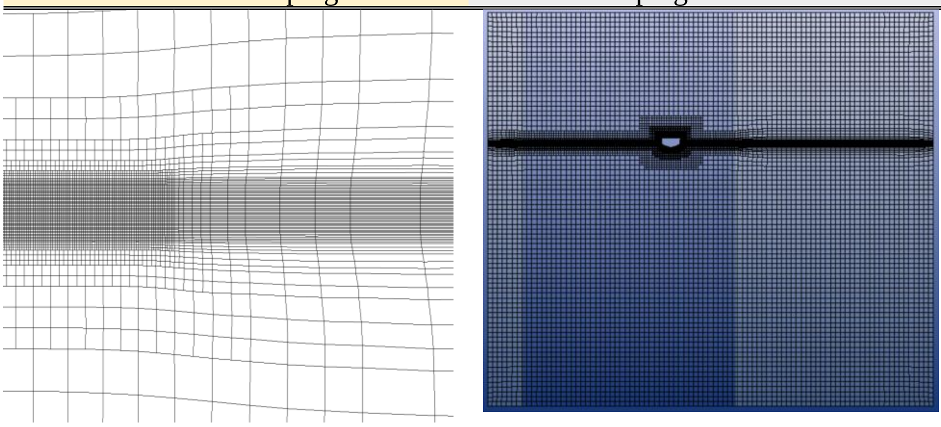

Figure 19. Damping Methods in FineMarine for seakeeping tests

7.1.2. *Viscous layer insertion*

In the present case, the viscous layer is the last process carried out in HEXPRESS. The procedure is through to use of ship speed and reference length to determine the Reynolds number. Since the solver uses Reynold average Navier-Stokes, the previous parameters of the Reynolds number are used to obtain the y^+ parameter to create a viscous layer. Figure 20 shows the transition in HEXPRESS from the initial mesh to the viscous layer insertion.

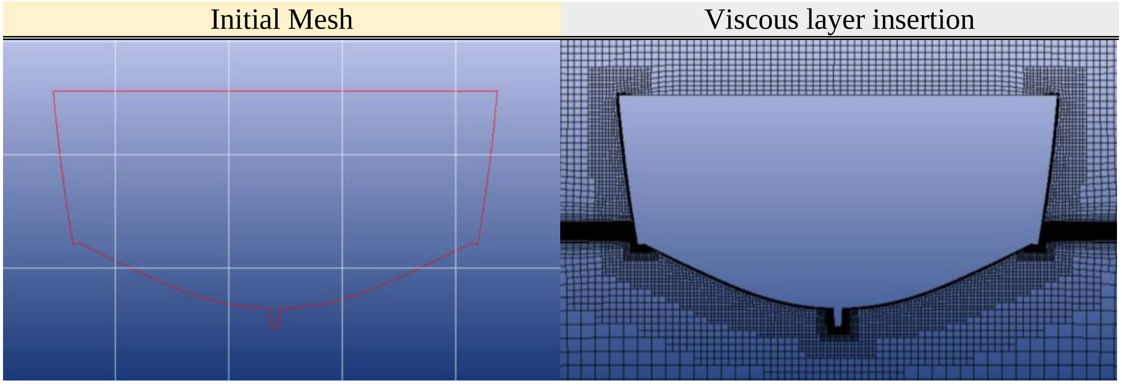

Figure 20. Mid-Ship section viscous layer comparison

7.2. Results at different wave amplitude

Figure 21 shows the RAO for three different input TWG using three different wave amplitudes. It is notorious that the responses are entirely different as long the amplitude changes. Also, the results on RW confirm the discrepancies in the answers. For example, with the wave amplitude 0.5 meters, the resonance frequency moves at a higher wave period in the roll RAO.

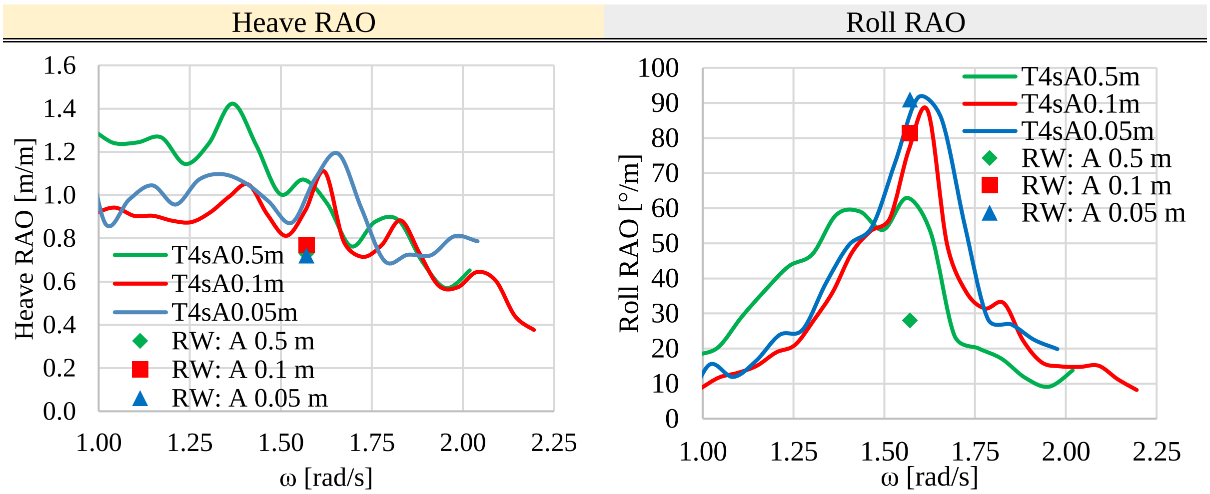

Figure 21. RAO comparison at different wave amplitudes in mid-ship section simulations

Figure 22 shows the mass flow of the simulations, where the nonlinear behavior is predominant at a wave amplitude of 0.5 meters. Besides, the figure illustrates the conduct at 0.1 and 0.05 meters in RW and TWG. The incidence of non-linearities is vital due to acceleration and smashing of the free surface and the bottom side. Therefore, TWG simulation is not accurate in this case due to the nonlinear environment. Consequently, the RAO in beam seas is susceptible to the input spectrum energy even with the same peak period.

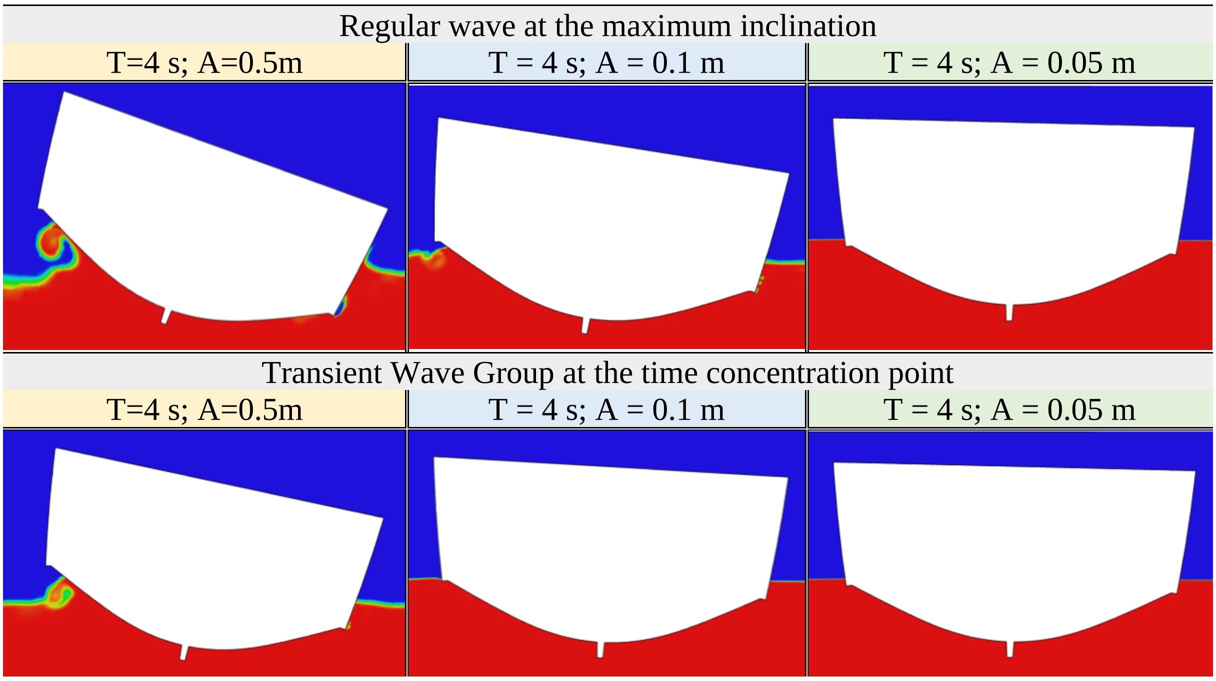

Figure 22. The mass fraction at a maximum inclination of a mid-ship section

Despite the non-linearities caused by the solid shape, the steepness wave is also a generator of non-linearities in the simulation. For this, Méhauté [9] graphic is used to determine the level of non-linearity using the wave characteristic. Consequently, Figure 23 shows the linearity of different wave amplitudes (with the same wave period of 4 seconds). Moreover, the results from Figure 21 have matched with the incidence of non-linearities in the wave characteristics. Therefore, in this case, it is recommended to use wave environments maximum to the second order of stokes waves to obtain decent results.

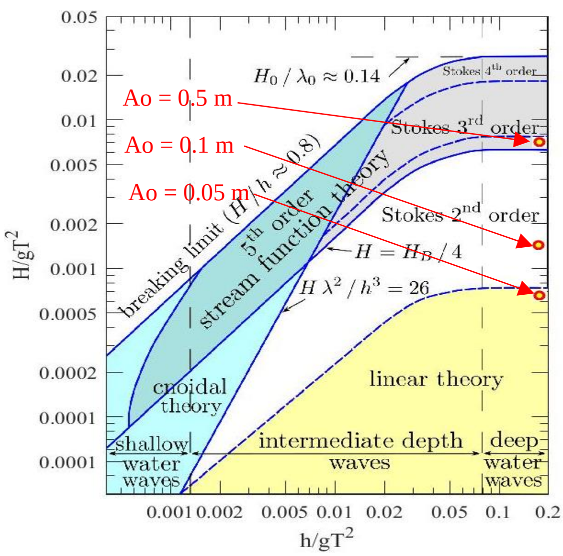

Figure 23. Méhauté graphic at the different wave amplitude in a 4 second wave periods [9]

7.3. Results at different wave peak period

This section performed three simulations with the same wave amplitude (5 cm) in three different peak periods. The RAO results, in Figure 24, presents excellent results in the case of roll RAO but with some discrepancies in the heave motion, but it is still a similar behavior. In addition, the result was validated with three regular waves in black points in the mentioned figure, showing acceptable results and behavior. Another comment, TWG method has accurate results near the peak frequency. Nevertheless, the results have instabilities if the frequency is far from the peak period.

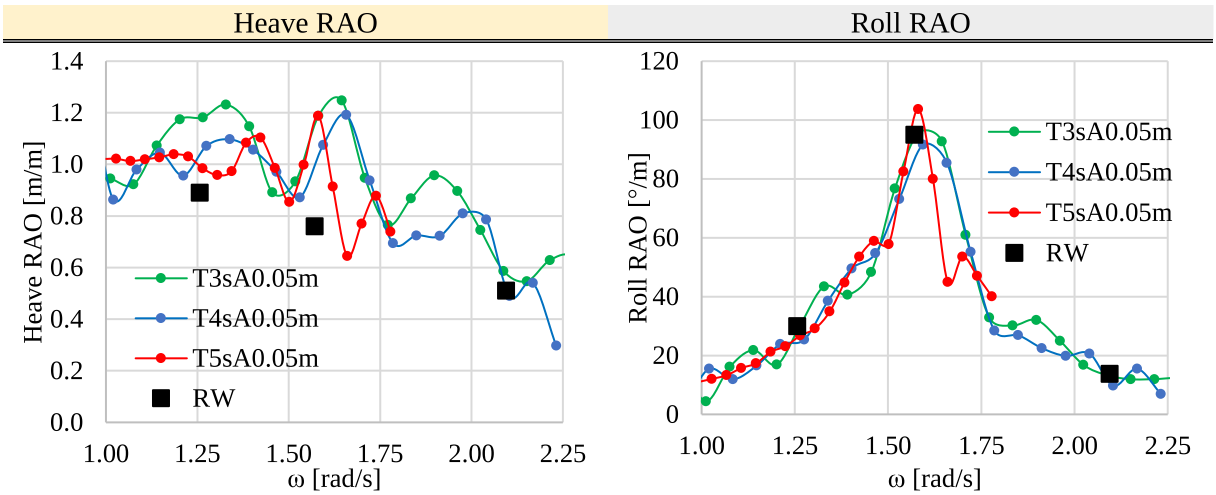

Figure 24. RAO comparison at different peak periods in mid-ship section simulations

In this case, the discrepancies and the non-smooth shape lie on the no-possibility of filtering post-processing data. The reason for the non-use of the Hann Filtering are:

- In the 2D case in FineMarine, it is impossible to obtain the FSE in the concentration point (longitudinal center of gravity). The domain at that point is empty. In this case, the wave spectrum used is theoretical, which leads to a non-accurate result.
- The low roll inertia value (beam seas simulations) produces long-time simulation to stabilize the roll motion. Thus, RAO magnitude changes due to the data's loss in long simulation. Besides, the long stabilized roll motion creates a reaction in the heave motion because both motions are coupled, as shown in Figure 25.

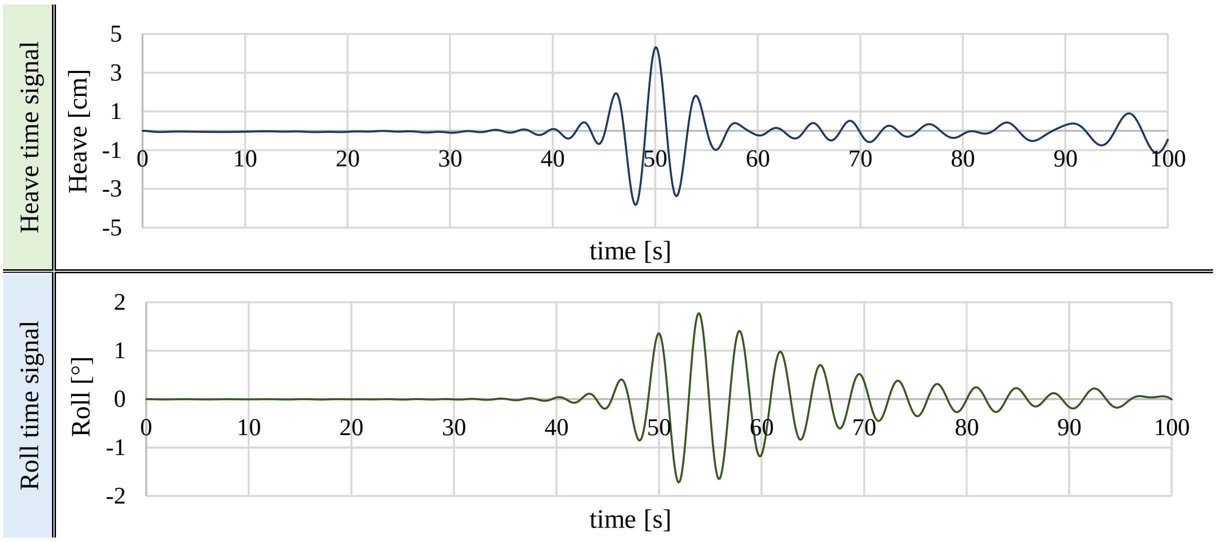

Figure 25. Time signal responses on mid-ship section with a TWG of T_p=4s and A_o=5cm

7.4. Multiple TWG simulation in a Mid-ship section

Multiple TWG input spectrum is a solution for the limit of the range of frequencies results. The current project used three different TWG energy of excitation, as shown in Table 7, to cover a wide range of frequencies. Also, it is noticing that the summatory of all the wave amplitudes results in 5 cm to avoid non-linearity due to the high steepness coefficient, as shown in Figure 26.

Table 7. Multiple TWG characteristics in Mid-ship section simulations

N°	T_p	A_o	s	Time Simulation
	[s]	[m]	[m^{-1}]	[s]
1	3	0.023	0.2	
2	4	0.017	0.08	120
3	5	0.01	0.05	

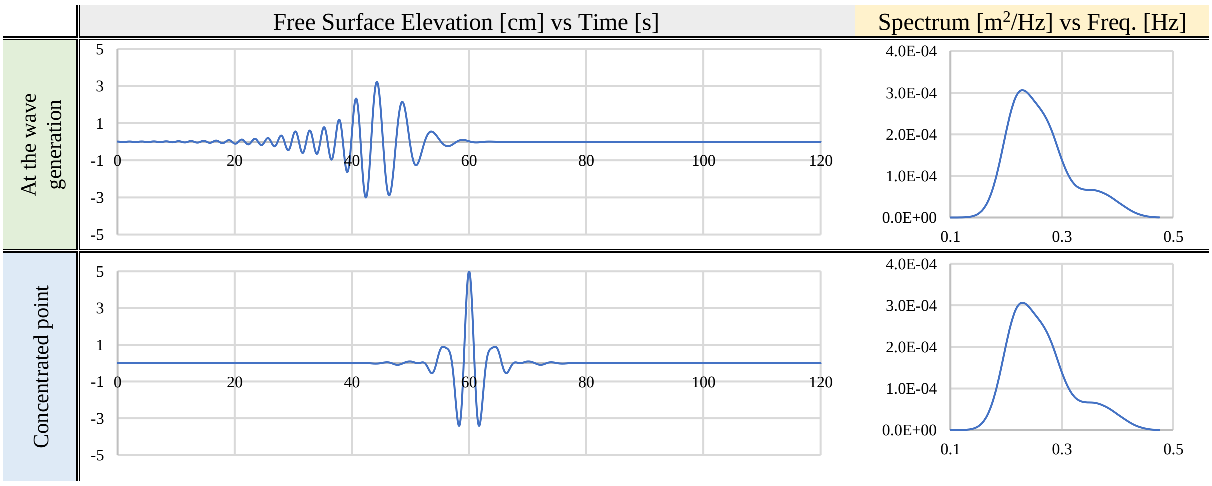

Figure 26. Input Spectrum of multiple TWG at mid-ship section simulations

The simulation results, in Figure 27, are compared with the simulation with one TWG of 4 seconds of the peak period. The RAO of this section and section 8.3 have acceptable results but discrepancies due to not including post-processing data. Besides, the figure plot three points obtained in RW simulations, and the tendency follows the TWG simulations.

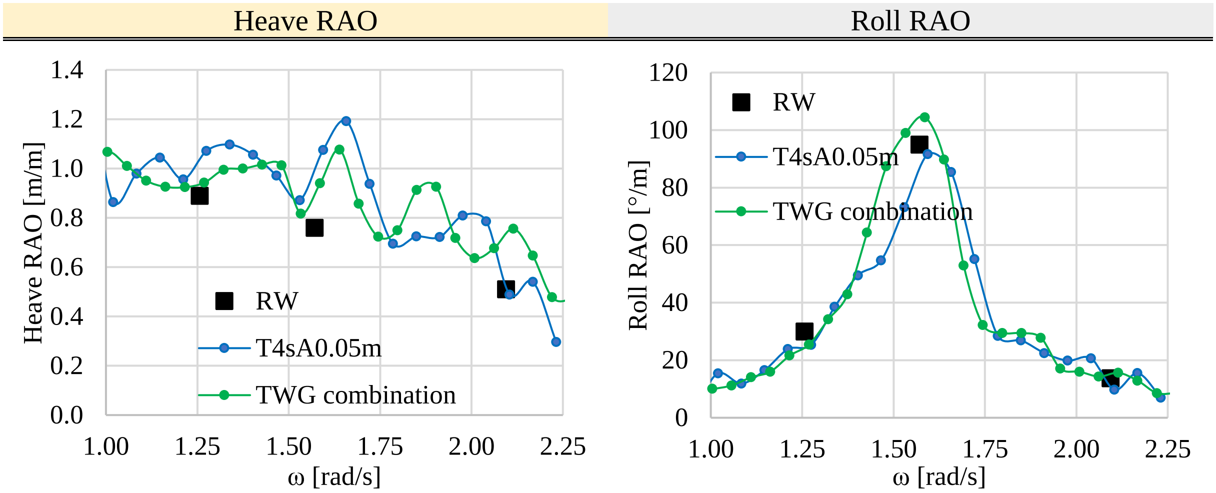

Figure 27. RAO results using a multiple TWG combination at the mid-ship section simulations

7.5. TWG computational time comparison

As a result, the RWs are faster simulations than the TWG method, and the time simulation depends on the stability of the response time signals. For another hand, the TWG simulations spend more time than RW. Still, it is possible to obtain more points in the RAO frequency domain than RW simulation. Figure 28 shows the comparison of the RW and TWG on this section using one conventional desktop.

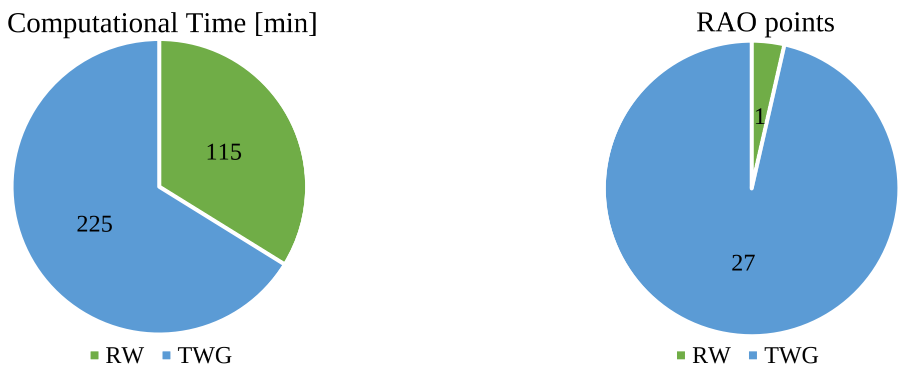

Figure 28. Comparison between TWG and RW simulations in stage 2

Finally, all the TWG simulations demonstrate a new technique on the seakeeping test in FineMarine CFD software. Despite the discrepancies, the results have equal behavior and assert to use TWG energy excitation in the 3D seakeeping test. Also, it expects accurate results in head seas 3D simulation because it is possible to use a filtering method in time signal responses.

8. THIRD STAGE: 3D – PATROL BOAT SEAKEEPING TESTS

Since the previous section asserts the use of TWG to obtain RAO with a simple 2D case, the consequence is the assertion to use the equal methodology in 3D simulations. Thus, the plan is to study a patrol boat of 80 meters in length of MAURIC design. Also, the provided experimental results are from a model with a scale ratio of 13.15. In addition, the simulation model uses the full scale without considering the propulsion system appendages. On the other hand, the model scale uses all the appendages (Bow thruster, Bilge keel, Spray rail, Rudder, Shaft line, Bearings). The main characteristics of the ship are shown in Table 8 and the 3D simulation model in Figure 29.

In the preliminary design stage, seakeeping test in software based on Potential Flow plays an essential role in the naval industry. That type of software obtains quick calculations to modify shapes until reaching the optimized model. Thus, using experimental tests or CFD simulations in the first non-optimized model is costly and time-consuming. Consequently, numerical and experimental simulations are the last step in the design process for verification data of the potential flow solver. Besides, Potential Flow is accurate at a relatively low-Froud number; that is why a simulation or experimentation is mandatory in the last design stage when the ship raises a higher speed.

Table 8. Principal particulars of the Patrol boat

Designation	Symbol	Magnitude
Main Particulars		
Length / Breadth ratio	L/B	6.27
Draught on AP / Breadth ratio	T_{AP} / B	0.05
Draught on FP / Breadth ratio	T_{FP} / B	0.29
Position of the center of gravity		
Long. center of gravity, aft to fwd / Length ratio	LCG / L	0.47
Vertical center of gravity / Breadth ratio	KG / B	4.65
Transversal center of gravity / Breadth ratio	TCG / B	0
Radius of gyration and inertia		
Mass radius of gyration around X axes	k_{xx} (% B)	35
Mass radius of gyration around Y axes	k_{yy} (% L)	22
Mass radius of gyration around Z axes	k_{zz} (% L)	22

Ship model of numerical simulation

Figure 29. Patrol boat comparison for the simulation and experimental seakeeping test

In this project, Qship is the potential Flow-based software to solve the seakeeping test. As a result, Figure 30 shows the preliminary results of the patrol boat without forwarding speed at different heading angles. Among the results, responses are predictable; for example, roll responses are more predominant in beam seas than pitch responses in head seas. Furthermore, these frequencies where the RAO is predominant serve as design input data (peak period) to create the TWG spectrum in FineMarine. Finally, the RAOs using Qship in the ship with velocity are plotted in Annex 1 and 2.

Qship seakeeping results without ship velocity

Heave RAO / Max(Heave RAO)	Pitch RAO / Max(Pitch RAO)	Roll RAO / Max(Roll RAO)

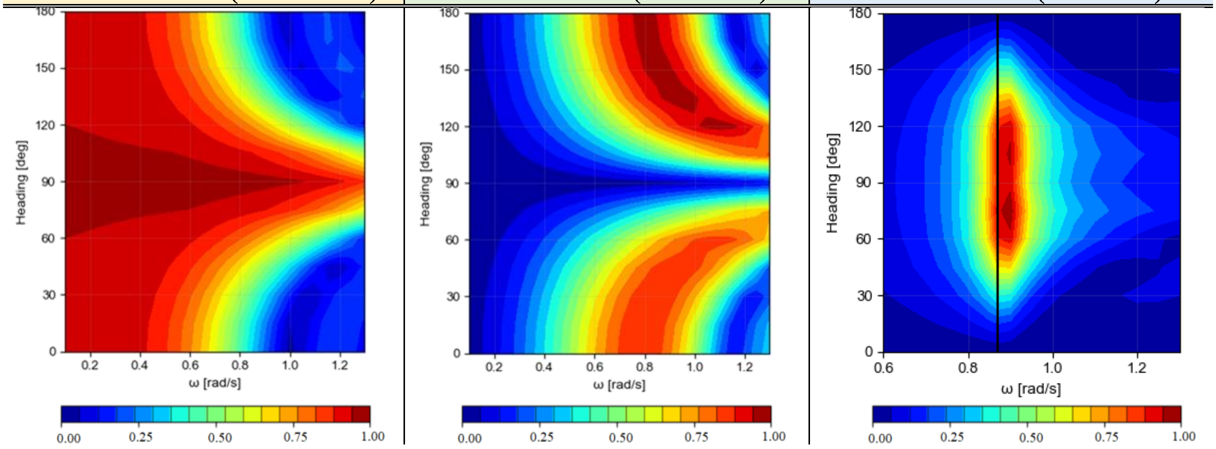

Figure 30. Qship results of RAO without of ship velocity

In the current stage, the simulations are performed to obtain the responses in beam seas ($\mu=90°$) and head seas ($\mu=180°$) respecting the heading convention in Figure 31. Those evaluations are the most important in ship design for the obtain more critical responses. As a reminder of the project's principal objective, the plan is to compare the simulation responses results with the experimental data and the data by Qship to validate the use of TWG.

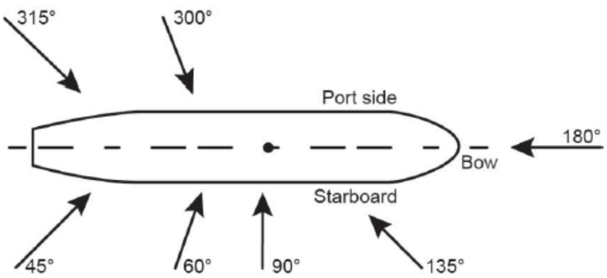

Figure 31. Heading angle convention, μ

8.1. Head Seas without ship speed

From Figure 30, the maximum responses in head seas occur with waves of 8.8 s (0.7 rad/s); that is the reason this is the main input parameter to design TWG. Besides, the other TWG parameters are 0.625 m of wave amplitude and 0.025 m^{-1} of standard deviation. This simulation takes all the parameters to consider the design domain, and the management set up in sections 5.2 and 5.4, respectively. Therefore, Figure 32 shows the input spectrum selected in the simulation with a simulation time of 200 seconds.

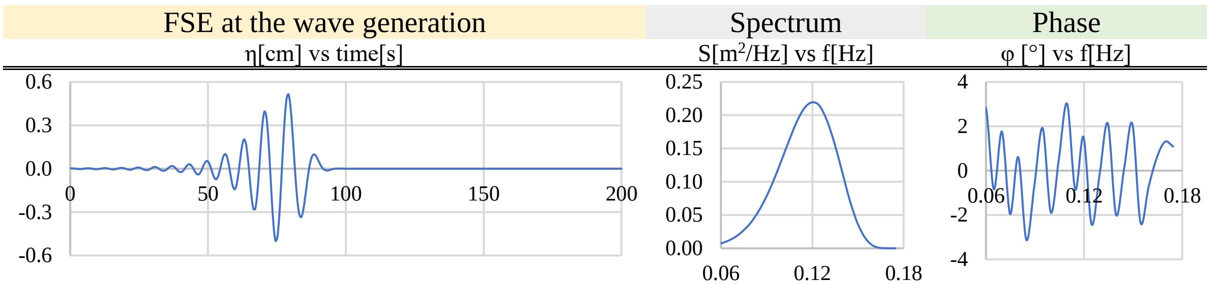

Figure 32. Input TWG spectrum of a patrol boat in Head Seas without ship velocity

8.1.1. Simulation time signal result

Figure 33 shows the theoretical and experimental FSE followed by the heave and pitch signal ship responses. It is evidence of some discrepancies between the theory and simulated FSE; the reason is the spectrum leakage in the wave generation. However, using a power two of Hann Filter deals with the differences after the concentration-time. Concerning the motions, the detail to recall is the faster stability of the pitch motion (in comparison with the 2D cases in stage 2) which helps to use filter tools and obtain a smooth RAO result.

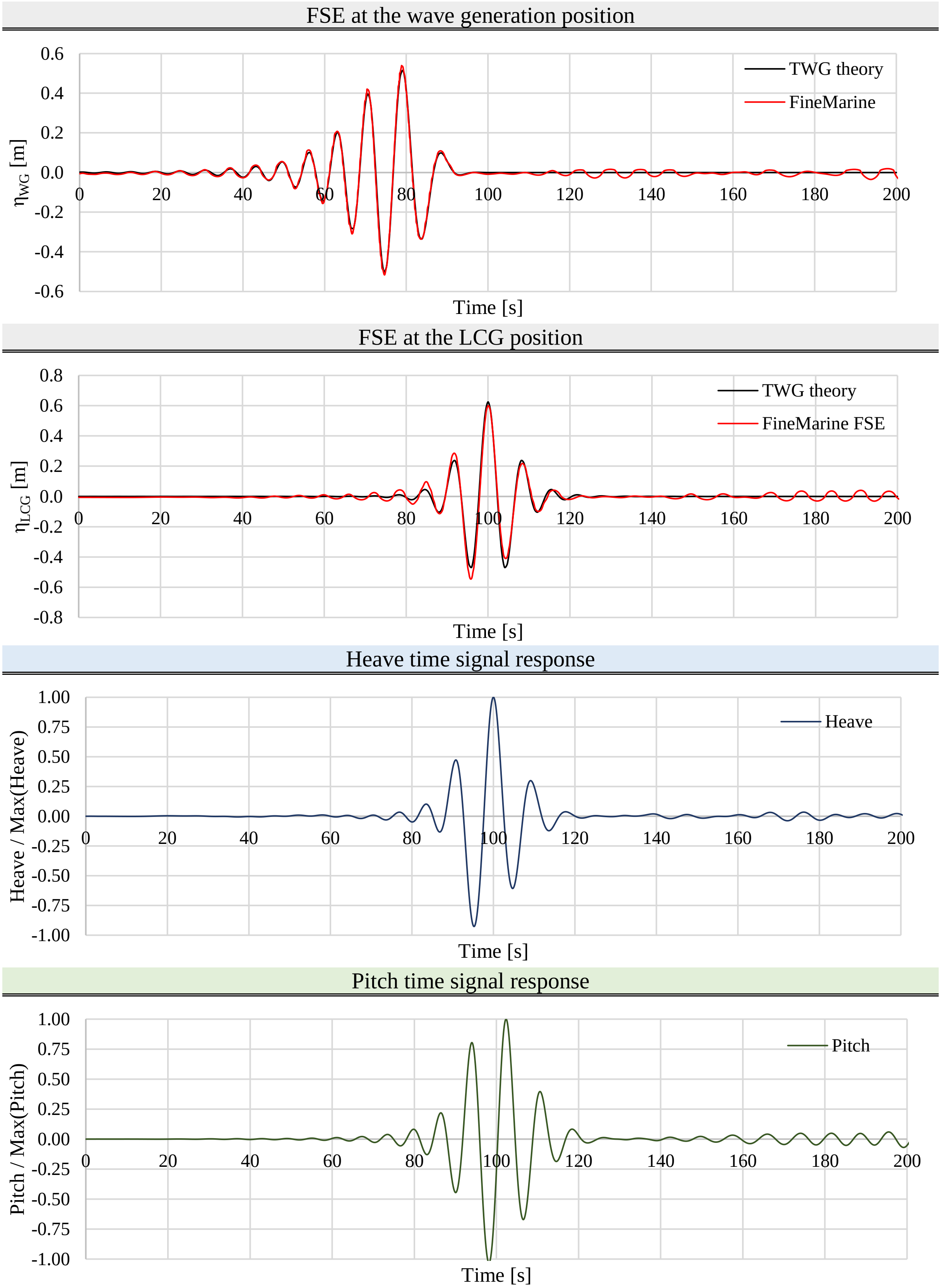

Figure 33. FSE and responses time signal for a Head Seas without ship velocity

8.1.2. RAO results

Using discrete-time Fourier transform in the FSE signal in the LCG position and Heave and Pitch signals, Figure 34 shows the spectrum necessary to calculate the RAO using Eq. 1. The figure affirms the importance of selecting a correct peak period in TWG using the data previously obtained in the Qship. The currently selected range of wave energy excitation brings enough frequency points to calculate good quality values of RAO.

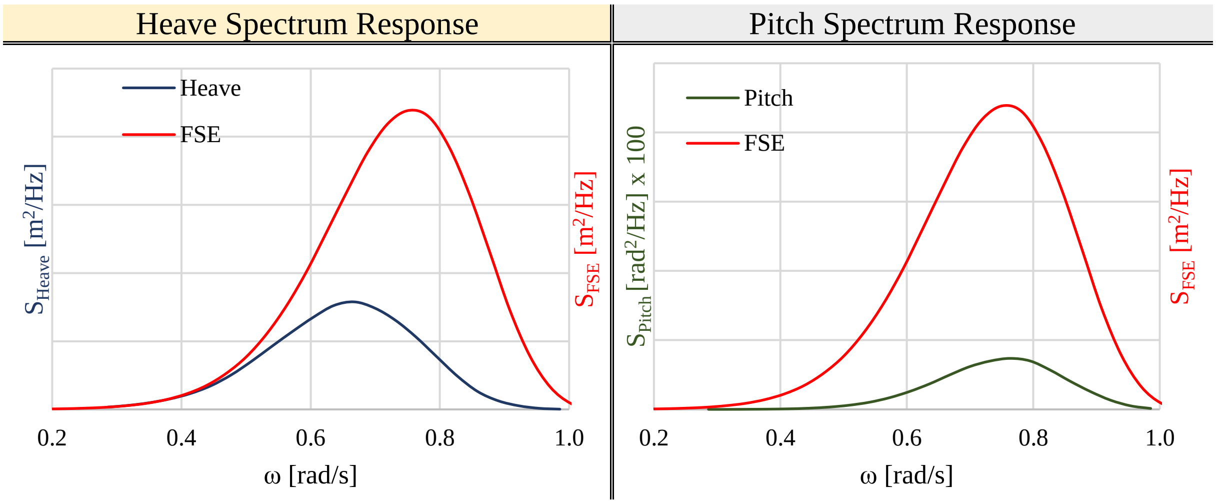

Figure 34. Responses Spectrum in Head Seas without ship velocity

Figure 35 shows the results of the seakeeping test of the ship without speed. The figure also compares the Qship responses with a successful outcome in RAO magnitude and behavior. In addition, there is no way to compare the results with the experimental data due to the lack of data in the only non-velocity case.

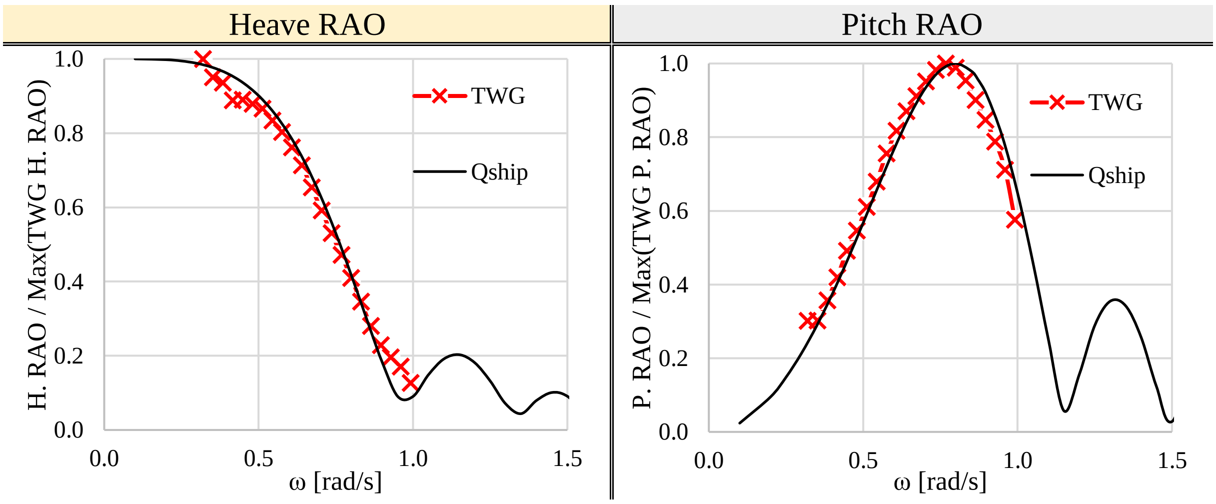

Figure 35. RAO in Head Seas without ship velocity

8.2. Head Seas with ship speed

Six and twelve knots are the corresponding ship velocities for the seakeeping simulation in this section. The speeds used for these simulations match with the data from experimental results. As the similar procedure of the previous section, using Qship, the input spectrum respects the range of maximums responses. The problem, in this case, is calculating the concentrated distance change on the setting TWG simulation with ship velocity. In Figure 36, the wave generation point seen in section 4.1 is changed due to the inclusion of ship velocity.

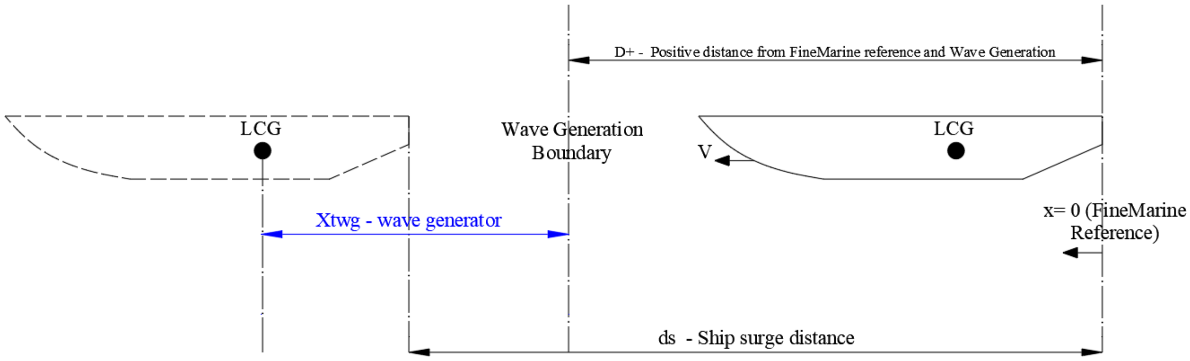

Figure 36. New distance of Wave generation input Spectrum in ship velocity

The procedure to obtain the new wave generation position (X_{twg}), from Eqs. 12-14, considers the parameters as the ship velocity (*V*), the domain, and the concentrated time ($2\ t_{/2}$), and the ship surge distance (d_s). In addition, a new term, t_{acc} in Eq. 13, is the time of acceleration where the ship takes to rise the steady velocity, which is proposed by NUMECA [6]. This new wave generation position is selected as an input value of TWG design.

$$X_{twg} = d_s - D^+ + LCG \tag{12}$$

$$t_{acc} = \begin{cases} 2.5 \cdot T_p;\ Fn>0.5 \\ V/0.2;\ Fn<0.5 \end{cases} \tag{13}$$

$$d_s = V\ t_{/2} - \frac{1}{2} V\ t_{acc} \tag{14}$$

Where:

- X_{twg} [m]; Final position of the wave generation in TWG design.
- d_s [m]; Total surge distance of the ship.
- D^+ [m]; Positive domain distance from the aft perpendicular to the wave generation.
- V [m/s]; Ship velocity.
- LCG [m]; Longitudinal center of gravity form aft perpendicular.
- t_{acc} [s]; Acceleration time in FineMarine.

- T_p [s]; Input TWG peak period.
- F_n [-]; Ship Froud number.
- $t_{/2}$ [s]; Half of the total simulation in TWG (concentrated time).

From the previous equations, one example of the input spectrum is in Figure 37. In conclusion, the position increases when the ship's velocity increases. On the other hand, in simulation without speed changes, the wave generation must create a wave pattern to generate an FSE required in the LCG position.

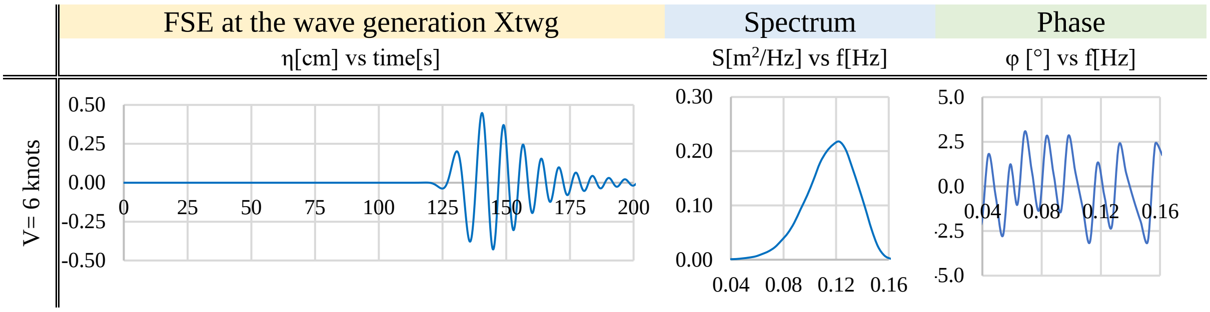

Figure 37. Input TWG spectrum of a patrol boat in Head Seas with ship velocity

8.2.1. RAO results

Before showing the results, the acquired data is received directly in the encounter frequency (ω_e). In this project, the spectrum responses, Figure 38, are shown in the encounter frequency domain. However, in Figure 39, the RAO uses the wave frequency (ω), using Eq. 14 to compare the frequency with the seawater spectrum. Additionally, the time FSE and responses signal of these two simulations is plotted in Annex 3 and 4.

$$\omega = \frac{1-\sqrt{1-4\omega_e \frac{V\cos\mu}{g}}}{2\frac{V\cos\mu}{g}} \tag{14}$$

Where:

- ω [rad/s]; Wave frequency.
- ω_e [rad/s]; Frequency of wave encounter.
- V [m/s]; Ship velocity.
- μ [°]; Heading of the ship, Figure 31.
- g [m/s^2]; Acceleration due to gravity.

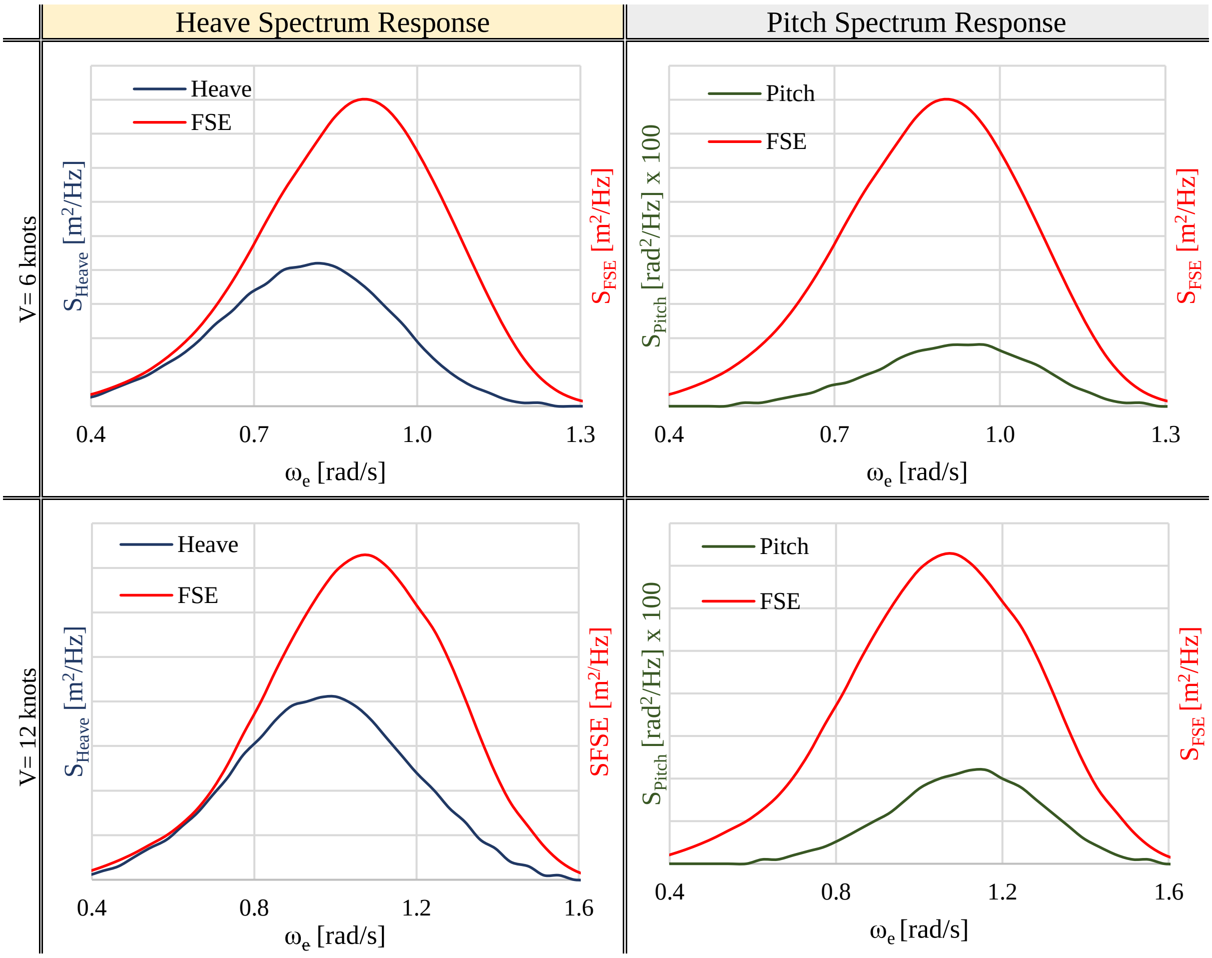

Figure 38. Responses Spectrum in Head Seas with ship velocity

Figure 39 shows the RAO response results compared with the Qship and the experimental data motive to mention the acceptance of the use of TWG in Head Seas Seakeeping tests. Besides, discrepancies can occur for the random wave energy in those kinds of tests.

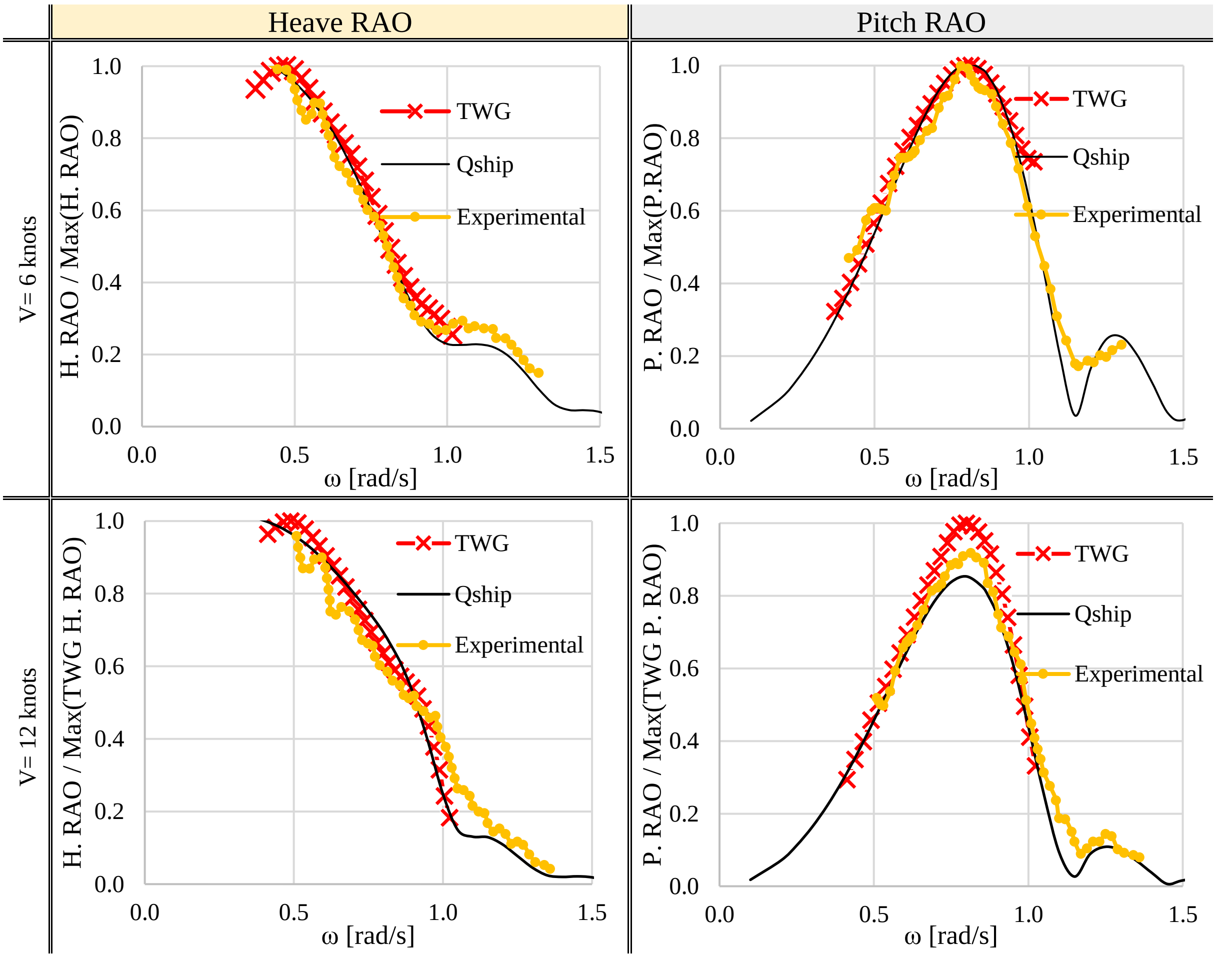

Figure 39. RAO in Head Seas with ship velocity

8.3. Beam Seas without ship speed

Figure 40 shows the input spectrum used in the simulation of beam seas without and with 6 knots of ship velocity. The effect of ship velocity with encounter frequency does not play in those simulations because the ship is navigating in a perpendicular direction (this corroborates the use of one input spectrum). The TWG uses a wave peak period of 7.2 seconds, a wave amplitude of 0.625 meters, and a standard deviation of 0.04 m^{-1}.

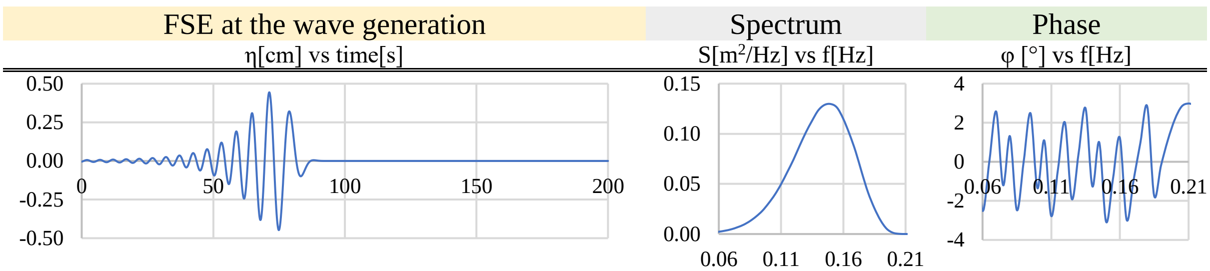

Figure 40. Input TWG spectrum of a patrol boat in Beam Seas

8.3.1. Simulation time signal result

Figure 41 shows the responses and FSE signal for the beam sea test without ship velocity. The reaction with 6 knots of ship velocity is shown in Annex 5. The results are affected by a reflected wave caused by the ship's surfaces. In addition, the non-real FSE produces inaccuracies in the RAO results. Besides, it is notorious, and the roll motions are not stabilized in the TWG time planned. With this, it precludes the use of filtering techniques.

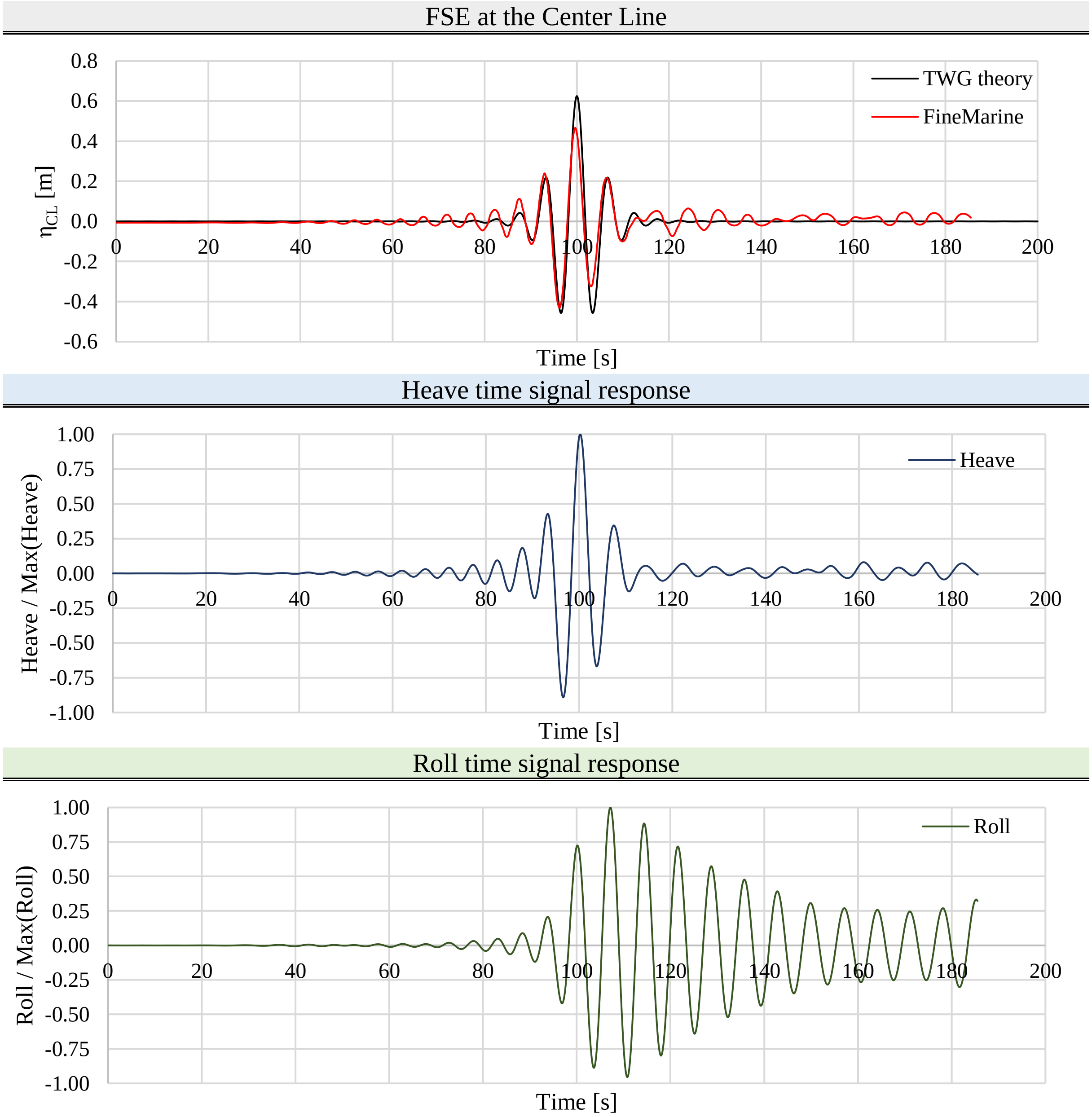

Figure 41. FSE and responses time signal for a Beam Seas without ship velocity

8.3.2. RAO results

Figure 42 is shown the response spectrum for both simulations. The results demonstrate the maximum energy frequency position but with different magnitude even in different ship velocities. Besides, it indicates that if the ship velocity increases, the damping effects in rolling increase. On the other hand, Figure 43 plots the RAO results with the evidence of non-accurate results, but it has the same magnitude in the roll motions. The response in heave motion without velocity does not obtain the expected results in the low-frequency range.

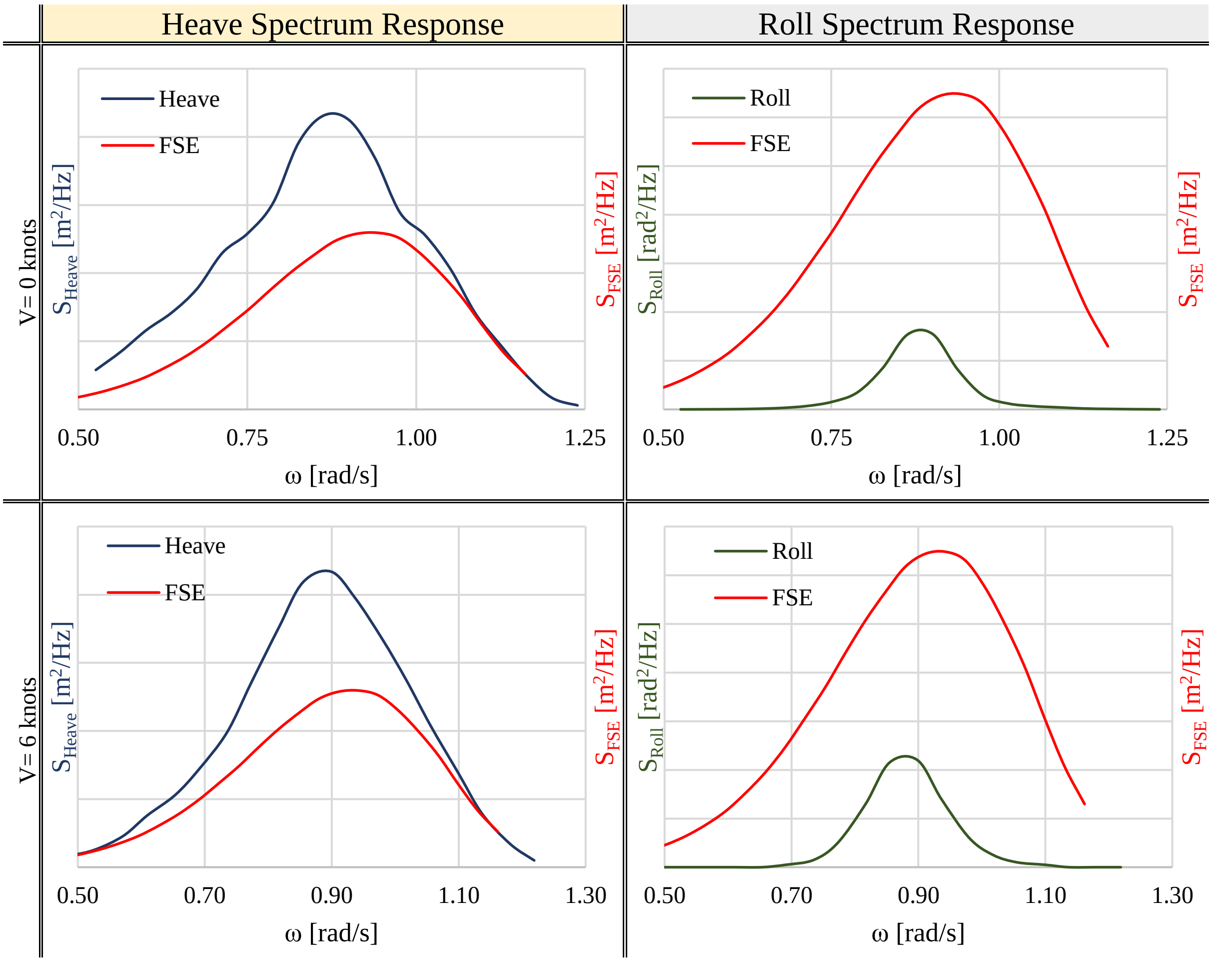

Figure 42. Responses Spectrum in Beam Seas

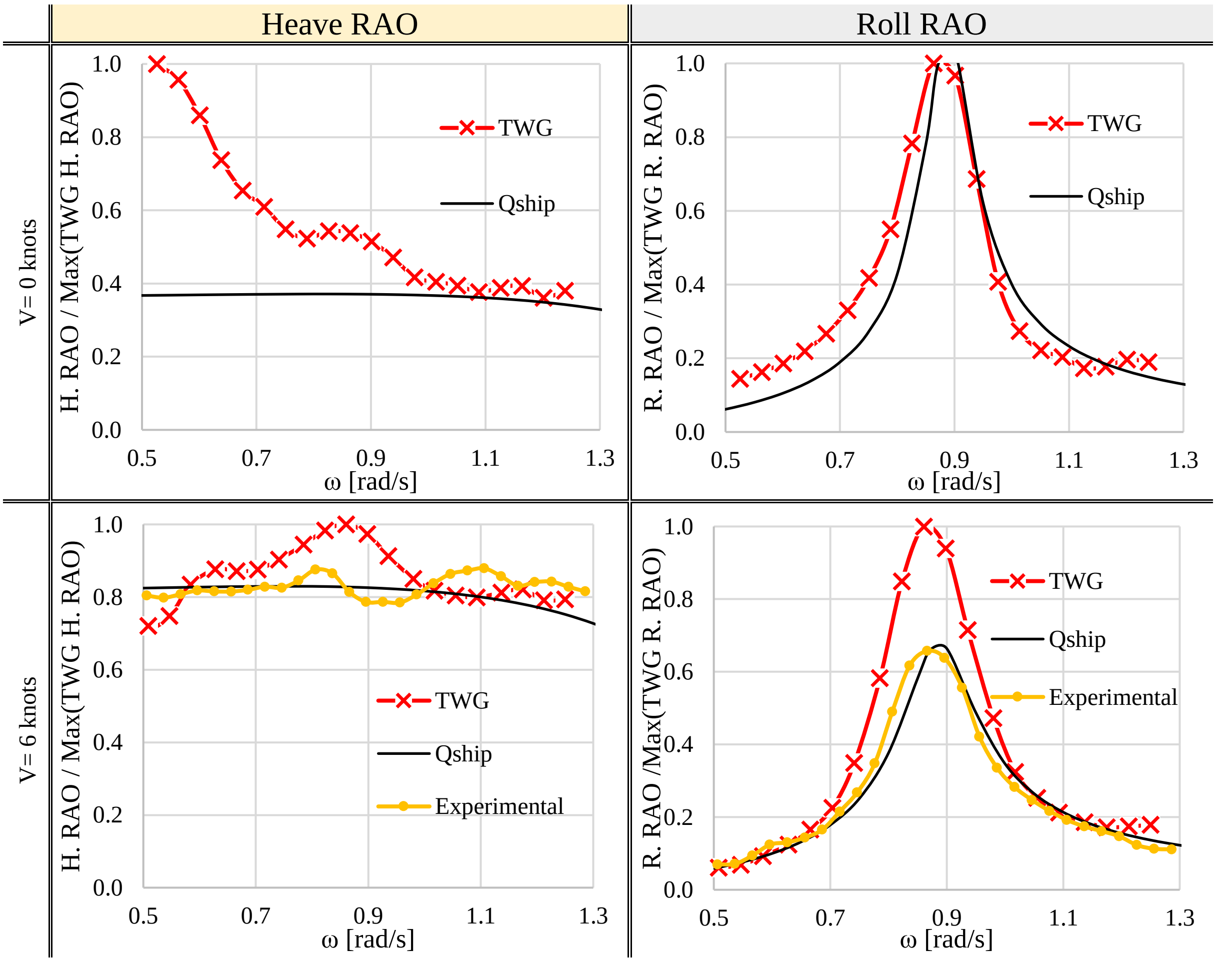

Figure 43. RAO in Beam Seas

8.4. CFD

The computational time and mesh can be summarized in Figure 44. Symmetry helps to decrease the number of cells in the case of head seas. On the other hand, beam seas require double cells than head seas, resulting in more computational time. Besides, the effect of continuous motion without stabilizing creates an increment of computational time as is placed in roll motion. In addition, the relatively high number of cells is related to the appendages used in the ship with the combination of quality mesh (using orthogonality cell greater than 10°).

Head Seas	Beam Seas
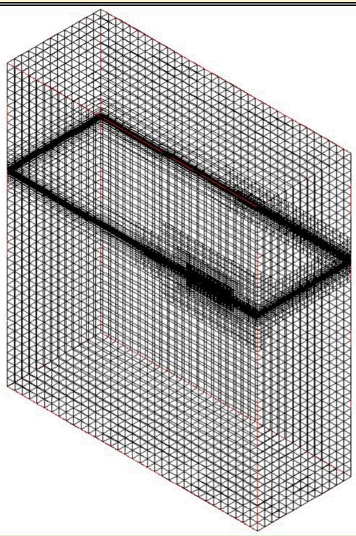	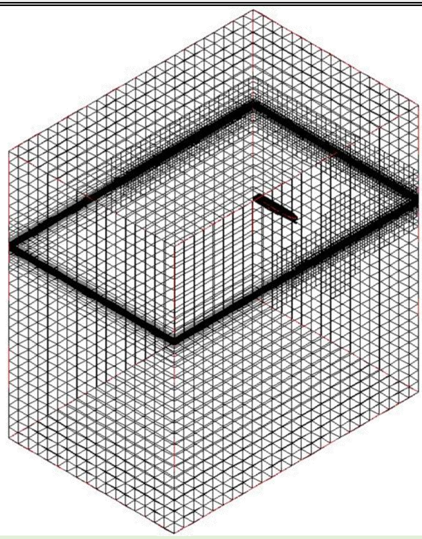
Number of the cell (approximation)	
6 million	12 million
Computer simulation time (approximation) with 128 cores resource	
25 hours	2.7 days

Figure 44. Domain Mesh and computational time in the Patrol Boat

In this project, the domain cell size is 19 m, the maximum solid cell size is 30 cm, and the minimum is 9 mm (without counting viscous layer insertion). In addition, Figure 45 and Figure 46 shows the following parameters used in the design of the mesh of the patrol boat:

- Use a refined mesh in the keel, bilge keels, leading and trailing edge of the rudder, and small surfaces.
- Use a refined mesh in the bow to adequately capture the FSE iteration in the simulation.
- Use of viscous Layer insertion in all the surfaces except for the deck area.

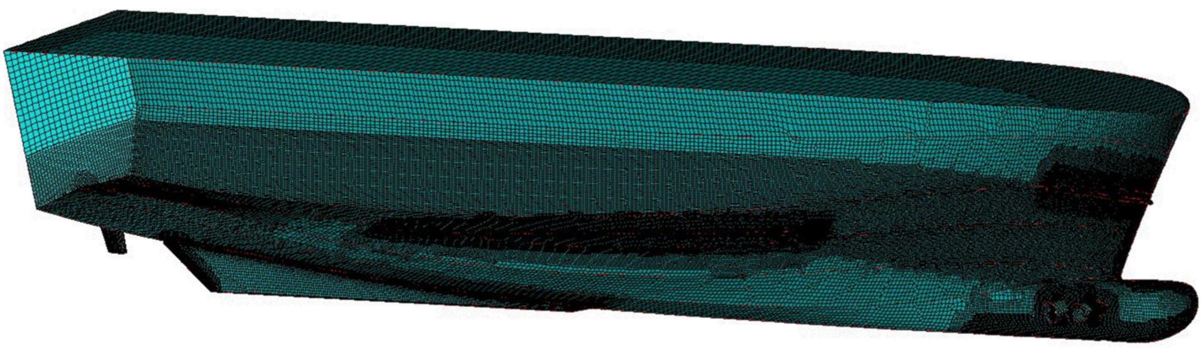

Figure 45. Solid Surface mesh in the Patrol boat of 80 meters length

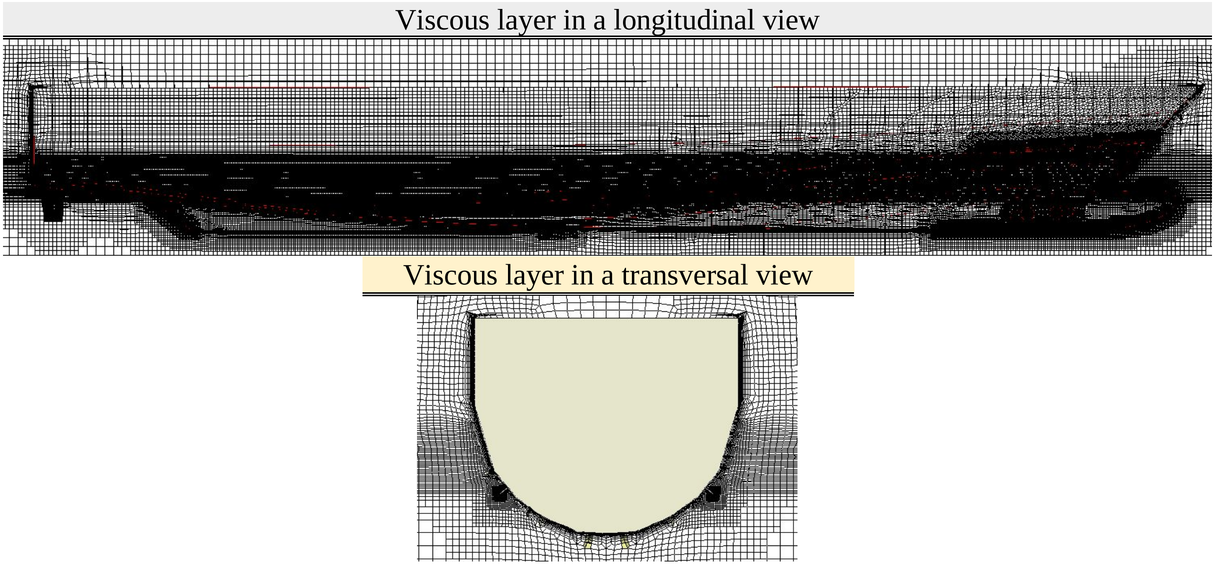

Figure 46. Viscous Layer insertion in the Patrol Boat of 80 meters length

Finally, Figure 47 shows one representation of the timeline simulation using CFview. Besides, the picture shows the ship going through the TWG at the concentration time and position in the Head Seas simulation. The ship's motion is not appreciable because the FSE appears only in a small range of time in the ship.

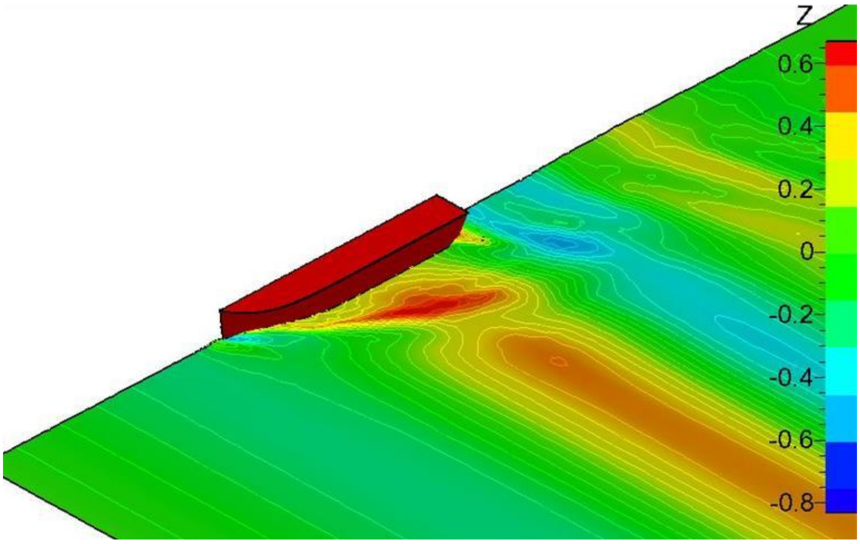

Figure 47. CFview of the current project in a TWG Head Seas simulation

8.5. Validation Seakeeping Tests

The Head Seas simulations have accurate results with the experimental data. However, in the case of beam tests, the responses must be analyzed separately due to differences. Figure 48 shows the relative error for the head seas test, where it is summarized:

- Without Ship Velocity: The base of the comparison is the Qship results. Also, it is essential to mention that there is a lack of information on the experimental test case that is why it is not considered in the analysis. The values show low error levels but with discrepancies as the frequencies move away from the original input peak period in the TWG design.
- 6 and 12 knots of ship velocity: Accurate results with less than 10 % error were performed. Nevertheless, the experimental result has irregular behavior in the relative error along with the frequencies. Besides, the experimental data use random phase waves, leading to a non-smooth shape and non-accurate results. Even if the same experiment irregular test is developed several times, it never obtains the same result.

Also, it is possible to determine the total mean value of error by root mean square (Table 9) using Eqs. 9-10. The equation requires choosing a base value; in the present case, the results provided by Qship in a low Froud number. As it is expected, the error obtained raises less than 13 % in the worst-case scenario. In conclusion, it is worth using TWG wave energy excitation to calculate the RAO in Head seas. Also, filter techniques are vital in this type of simulation due to spectrum leakage or reflected waves captured by the FSE readers.

Table 9. Normalized Root Mean Square Error for Head Seas simulations

Normalized Root Mean Square Error [%]						
Head Seas	Heave RAO			Pitch RAO		
	TWG	Qship	Experimental	TWG	Qship	Experimental
0 knots	3.1%	Reference	-	4.8%	Reference	-
6 knots	5.9%	3.3%	Reference	4.1%	4.0%	Reference
2 knots	8.5%	9.2%	Reference	13.0%	4.7%	Reference

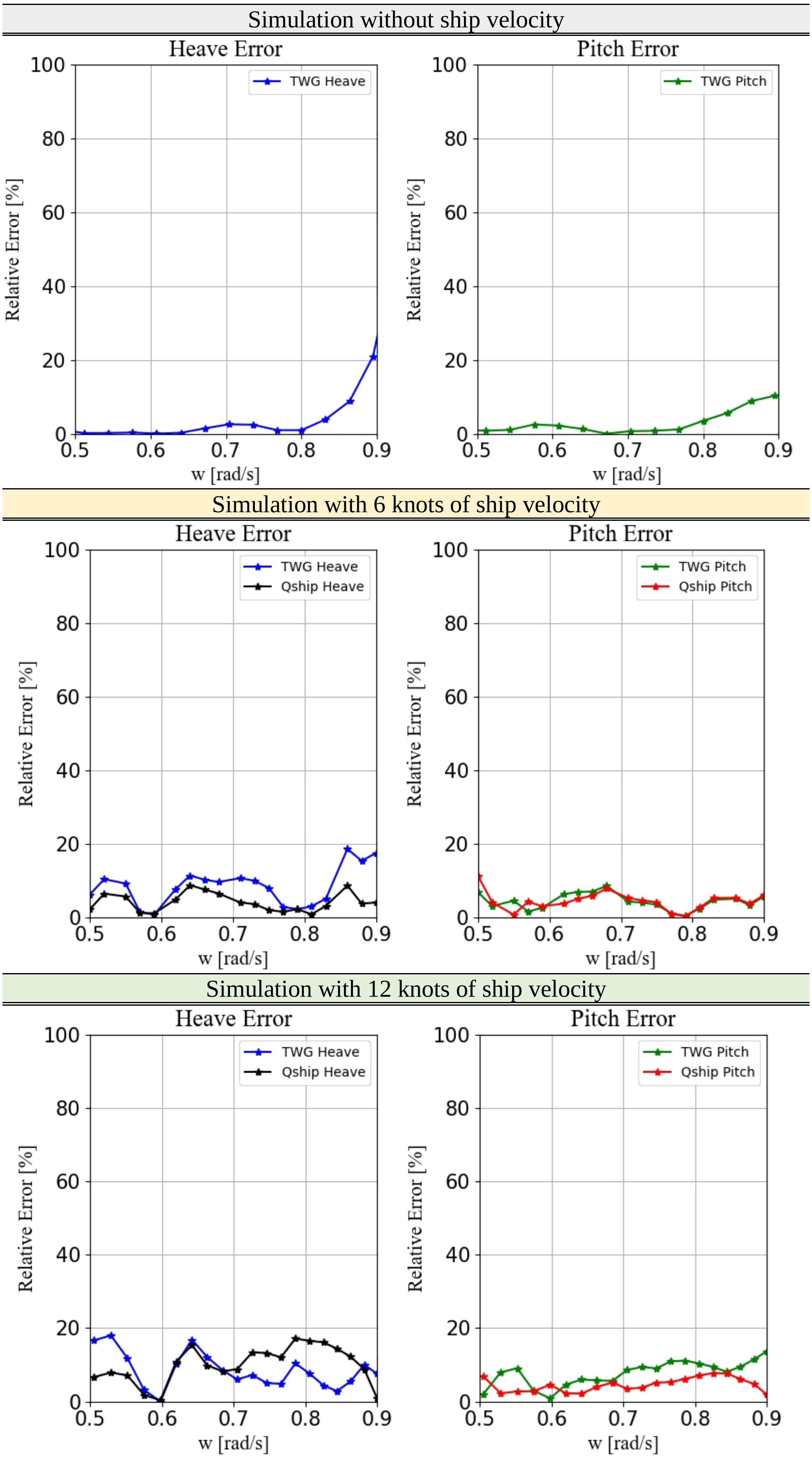

Figure 48. Relative error along with the frequencies in Head Seas tests

Now with the results in the simulations in beam seas, it is noticeable that it has a significant difference between the results proposed in TWG, in the relative error in Figure 49. In this case, it is essential to mention in the same way used in the case of section 8 (2D point in beam seas):

- The ship's response in beam seas depends on the amplitude of the wave used, and this can provide damping effects caused by the shapes of the solid, as seen in Figure 22. Furthermore, wave steepness plays a crucial character because it affects the nonlinear behavior of the TWG creation.
- Compared to the conventional spectrum in seakeeping tests, the magnitude of the spectrum is different in TWG. Even if the same input spectrum data is selected, the magnitude of energy changes. That is the reason the experimental result does not match the TWG data. In addition, it fits with the conclusion of section 7 (beam seas simulations), where RAO depends on the sea state as the input spectrum.
- The simulations obtained tend to be more susceptible to process. In the current project, with the proposed time, the rolling motion is not stable, and this causes problems in the use of filter techniques. A solution for this is to let the simulation continue until the roll stabilizes. Nevertheless, as at the beginning of the project, the objective is to reduce the simulation time of the proposed method.
- In 2D, better resolutions were achieved considering that the domain used is the internal wave generation. This case, which is feasible only for a boat without speed, is conducive to eliminating the waves reflected by the ship side and consequently having a better result.

As well as the relative result error, the overall mean errors, in Table 10, shows the error advance more than 10%. In this case scenario, it cannot be asserted the use of TWG but, considering the use of more time simulation; the simulation may obtain accurate results.

Table 10. Normalized Root Mean Square Error for Beam Seas simulations

Normalized Root Mean Square Error [%]						
Beam Seas	Heave RAO			Roll RAO		
	TWG	Qship	Experimental	TWG	Qship	Experimental
0 knots	31.3%	Reference	-	9.2%	Reference	-
6 knots	9.6%	4.7%	Reference	21.5%	4.8%	Reference

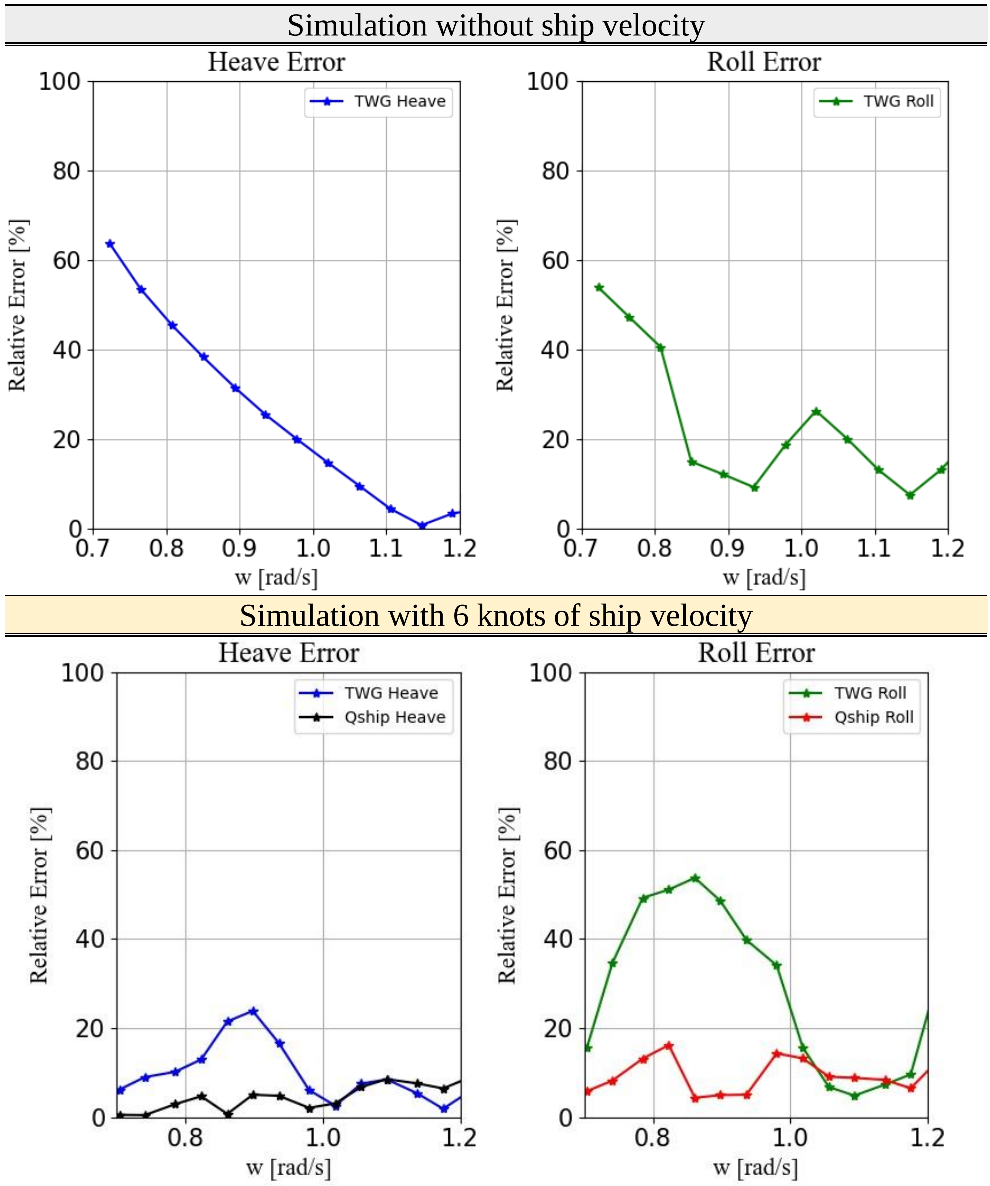

Figure 49. Relative error along with the frequencies in Beam Seas tests

Finally, it is necessary to emphasize the power of the transient wave group method, as shown in Table 11. This table compares the simulation time in the conventional test with the proposed TWG method. Also, it is adapted with the equivalence in time step in traditional seakeeping of CFD test. The result is encouraging since the use of TWG saves us 95% of the time steps provided by the conventional JONSWAP spectrum.

Table 11. Time step comparison between simulation using JONSWAP and TWG spectrum

Condition	Head Seas			Beam Seas	
Ship velocity	V = 0 knts	V = 6 knts	V = 12 knts	V = 0 knts	V = 6 knts
Irregular Wave Spectrum					
Simulation time	4400	4400	4400	4400	4400
Equivalent time steps	100000	100000	100000	100000	100000
TWG					
Simulation time	200	226	242	200	200
Time steps	4545	5146	5491	5556	5556
Time step Reduction	-95%	-95%	-95%	-94%	-94%

9. CONCLUSIONS

The project asserts the process in three steps to optimize the simulation time in seakeeping tests. Therefore, using the theory of Transient Wave Group proposed by Clauss and Bergmann [3], simulations in FineMarine software were performed with successful results. The free surface elevation, the simplified ship section, and the patrol boat simulations were validated with regular waves simulations, experimental results, and potential flow solver. However, it is essential to mention that the project has considerable discrepancies in beam seas simulations. After the analysis of the tests, the conclusions are:

1.- The boundary wave generation in FineMarine produces the same input spectrum with the theory's reliability on TWG. Even though there are discrepancies, either by the spectrum leakage or wave reflections FSE lectures, the obtained spectrum is the required for the test. In any case, the use of filter techniques helps to use the post-processing data to decrease the error and improve the spectrum shape.

2.- The midship section simulation performs decent results in the environment of linear waves. Using waves parameters in the ambit of the second order of Stokes' theory, the TWG result expects with the obtained in regular waves simulations. However, from here, it can be concluded that the RAO in beam seas depends on the input wave spectrum and the shape of the hull (it may create nonlinear wave breaking)

3.- The patrol boat succeed in the three planned simulations in Head Seas tests. With a maximum error of 13%, using TWG in the Head Seas simulation is optimum to reduce the computational time in the conventional seakeeping test. Even though the maximum speed is relatively low, the responses follow the results by Qship and experimental results.

4.- The patrol boat in the Beam Seas simulation is subjected to interpretation. The low inertia value produces a long time until the ship stabilizes in the roll motion. It is the case of the non-use of filtering techniques due to loss of measurements in response. As the second conclusion, the RAO beam seas depend on the input spectrum. That is one robust explanation of the difference between the experimental results and Qship solver.

10.ACKNOWLEDGMENTS

This thesis is dedicated to God and my family, who gave me their full and unwavering support without their presence. Rafael, Kathya, Ruth, and Carla, my beloved family, are entirely part of this thesis.

In addition, I would love to show my great appreciation to the people who permitted me to demonstrate my skills.

- Professor Philippe Rigo allowed me to be an EMship+ student. He guide and assistance in every challenge of the master program.
- Nolwenn de Kermadec and Antoine Durat were my supervisors during the master thesis period. They train and encourage me to be a better engineer in every step and objective of this master topic.

Finally, I would like to give my complete gratitude and admiration to the MAURIC company and Vincent Seguin for opening the doors of this internship. I have been very welcome and have had a great working environment every day.

11.REFERENCES

[1] M. C. Davis and E. E. Zarnick, "Testing ship models in Transient waves," *Fifth Symposium on Naval Hydrodynamics*, 1964.

[2] S. Takezawa, "A practical method for testing ship models in transient water waves," *JSNA*, vol. 128, pp. 119-132, 1970.

[3] G. Clauss and J. Bergmann, "Gaussian wave packets - a new approach to seakeeping tests," *Applied Ocean Research*, pp. 190-206, 1986.

[4] S. Mousaviraad, P. M. Carrica and F. Stern, "Development and validation of harmonic wave group single-run procedure for RAO with comparison to regular wave and transient wave group procedures using URANS," *Ocean Engineering*, no. 37, pp. 654-666, 2010.

[5] G. Ducrozet, Water Waves and Sea States Modelling - Statistical models, Nantes: Ecole Central de Nantes, 2020.

[6] NUMECA, "NUMECA documentation platform," NUMECA International, 2020. [Online]. Available: https://portal.numeca.be/docs/Default.htm. [Accessed 1 05 2021].

[7] C. Windt, J. Davidson, P. Schmitt and J. V. Ringwood, "On the Assessment of Numerical Wave Makers in CFD Simulations," *Journal of Marine Science and Engineering*, vol. 7, no. 47, pp. 1-45, 2019.

[8] NumPy, "numpy.hanning — NumPy v1.21 Manual," The NumPy community, [Online]. Available: https://numpy.org/doc/stable/reference/generated/numpy.hanning.html. [Accessed 01 05 2021].

[9] B. Le Méhauté, An introduction to Hydrodynamics and water waves, Pasadena, California: Springer science + Business media, 1976.

ANNEX

Qship seakeeping RAO result

Annex 1.- Qship Seakeeping results at 6 knots of ship velocity

Qship seakeeping results with 6 knots of ship velocity		
Heave RAO / Max(Heave RAO)	Pitch RAO / Max(Pitch RAO)	Roll RAO / Max(Roll RAO)

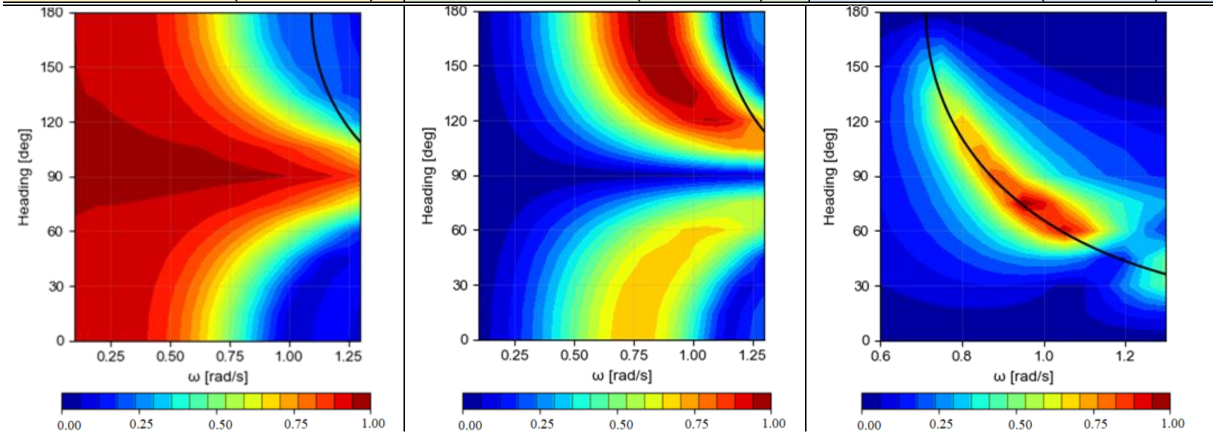

Annex 1. Qship results of RAO with 6 knots of ship velocity

Annex 2.- Qship Seakeeping results at 12 knots of ship velocity

Qship seakeeping results with 12 knots of ship velocity		
Heave RAO / Max(Heave RAO)	Pitch RAO / Max(Pitch RAO)	Roll RAO / Max(Roll RAO)

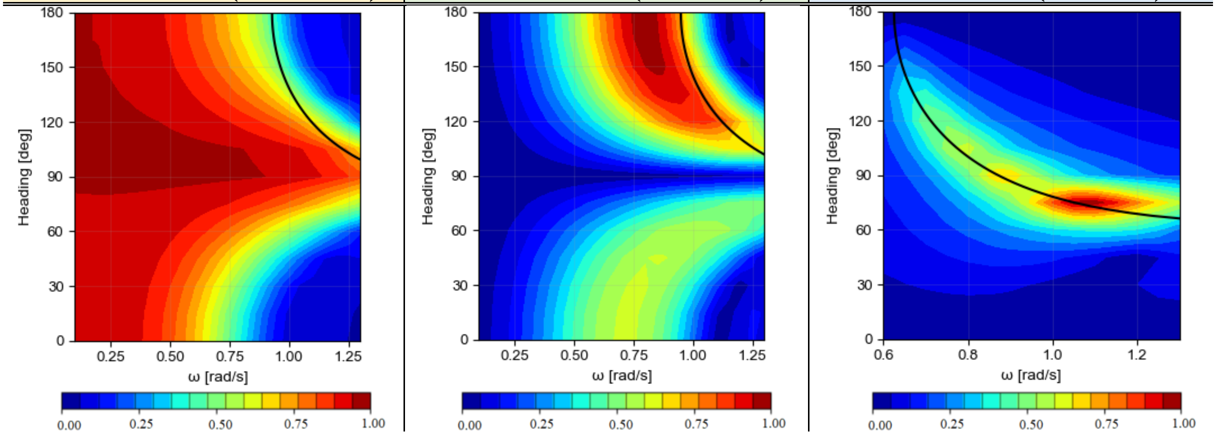

Annex 2. Qship results of RAO with 12 knots of ship velocity

Responses signal simulation results

Annex 3.- Responses' signal in Head Seas with 6 knots of ship velocity

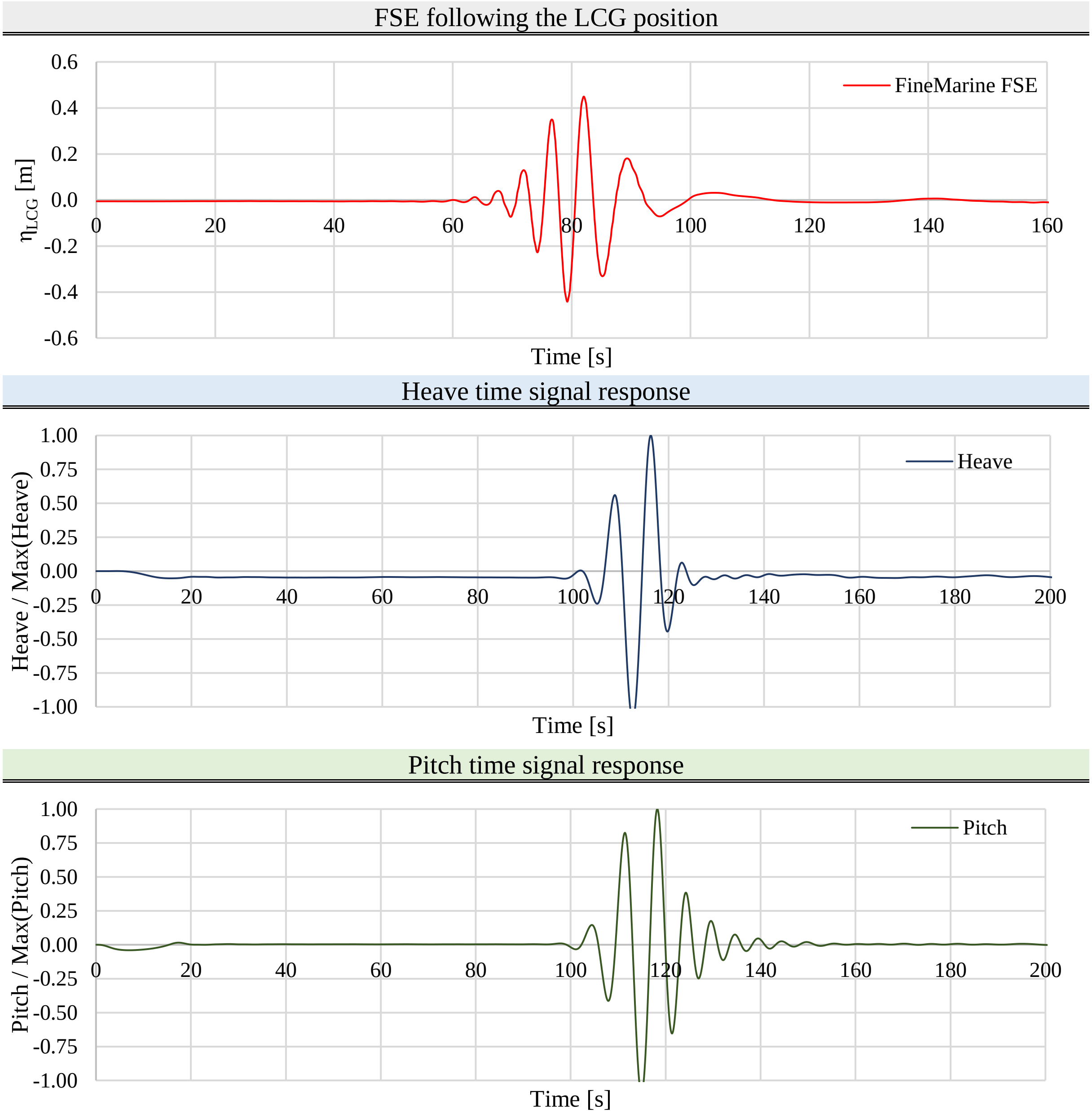

Annex 3. FSE and responses time signal for a Head Seas with 6 knots of ship velocity

Annex 4.- Responses' signal in Head Seas with 12 knots of ship velocity

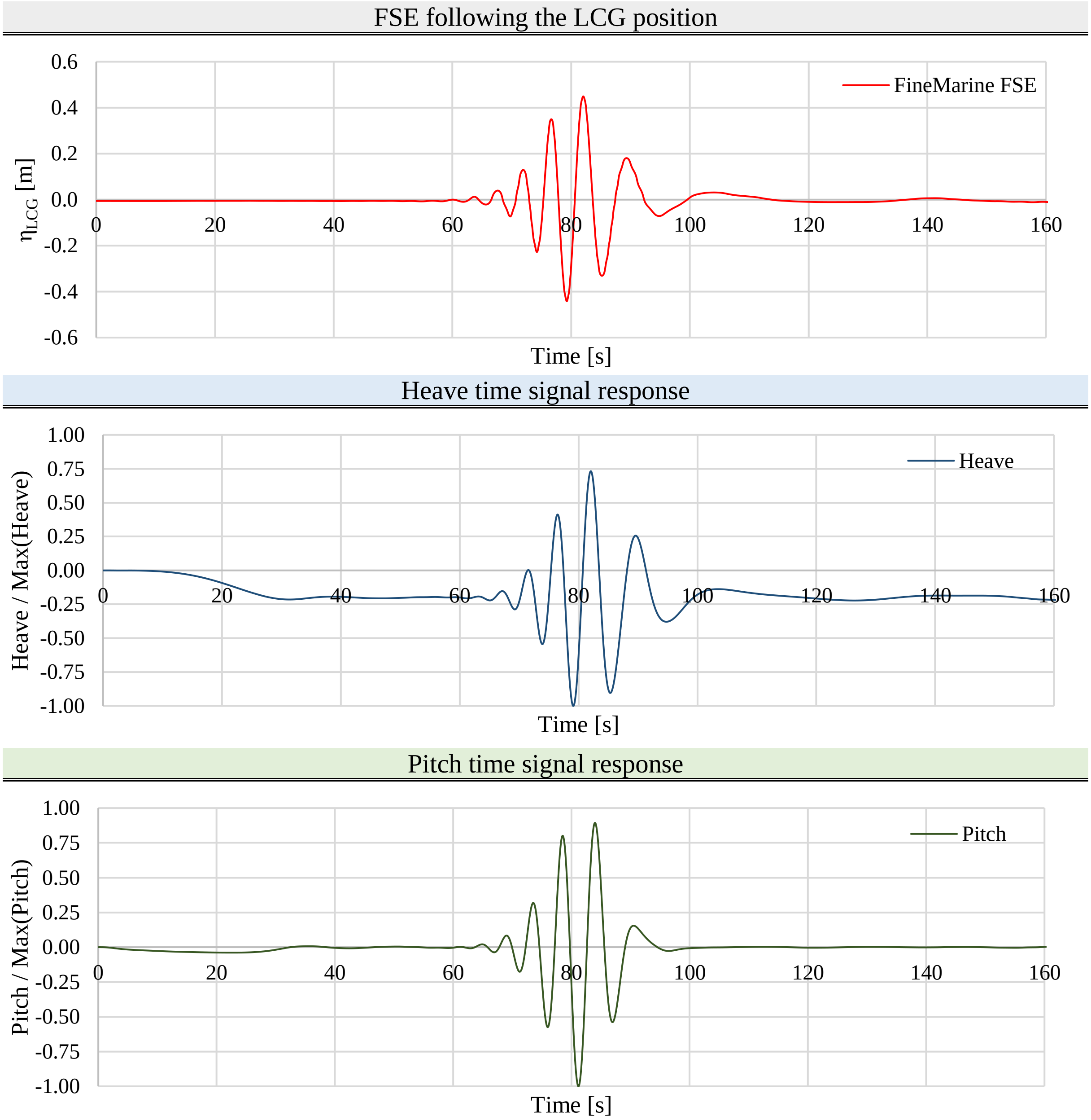

Annex 4. FSE and responses time signal for a Head Seas with 12 knots of ship velocity

Annex 5.- Responses' signal in Beam Seas with 6 knots of ship velocity

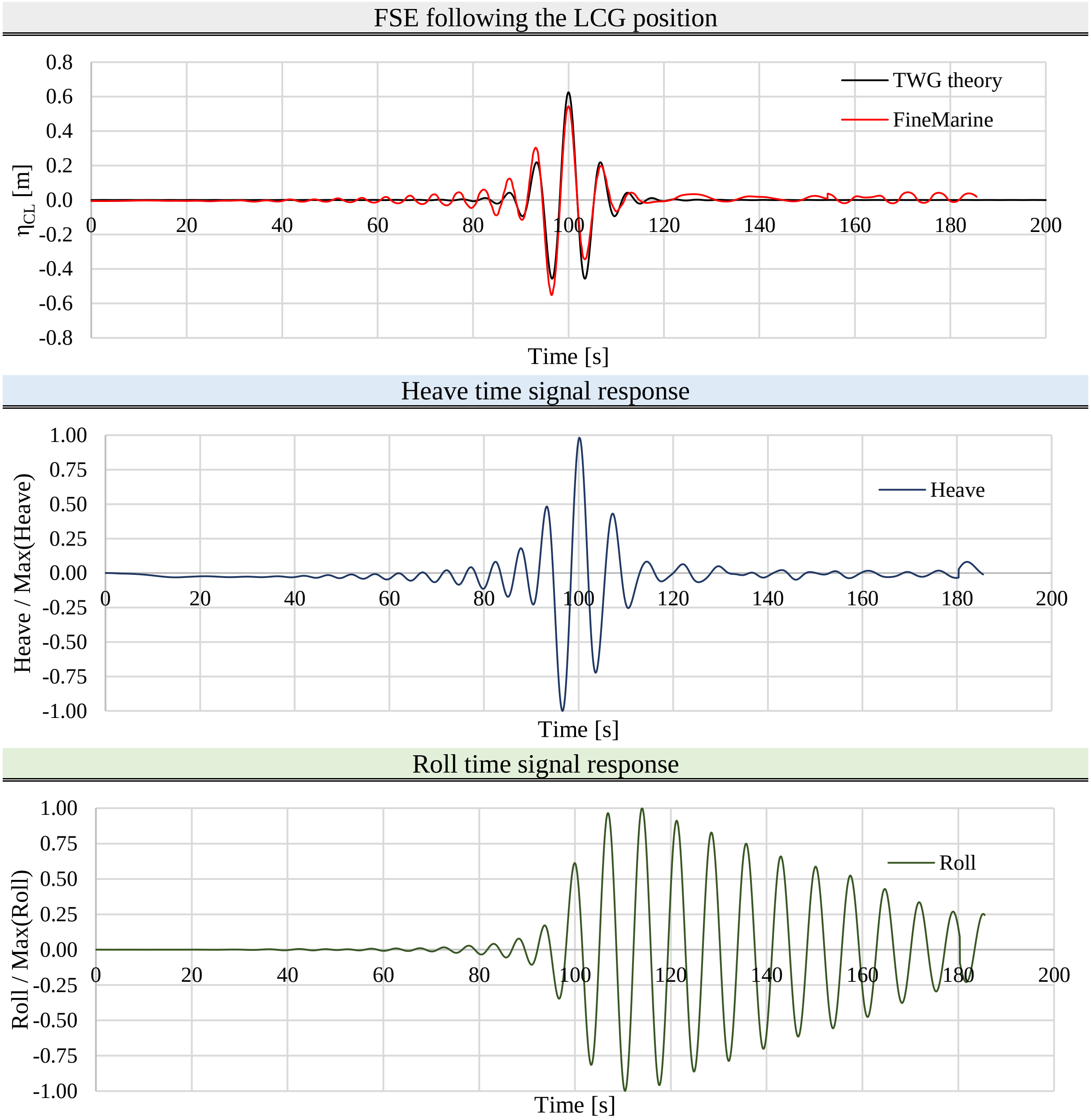

Annex 5. FSE and responses time signal for a Beam Seas with 6 knots of ship velocity